CALIFORNIA INSTITUTE OF TECHNOLOGY
Division of Physics, Mathematics, and Astronomy

FINAL TECHNICAL REPORT

to the

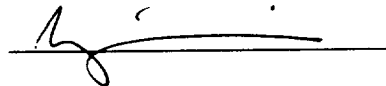**NATIONAL AERONAUTICS AND SPACE ADMINISTRATION**

for

NASA GRANT NAG5–4890

J. Zmuidzinas, Principal Investigator

Quasi-Optical SIS Mixer Development

Submitted by:

J. Zmuidzinas
Principal Investigator
Professor of Physics
Caltech, 320–47
Pasadena, CA 91125
(626) 395–6229
jonas@submm.caltech.edu

Contents

QUASI–OPTICAL SIS MIXER DEVELOPMENT

1 Introduction

This is the final technical report for a three–year grant NAG5–4890 which was awarded through our proposal to the NASA Research Announcement NRA–96–OSS–07–010. The funding start date was April 1, 1997, and the grant expired on June 30, 2000. The first two years of the grant were fully funded; the third year was only partially funded due to budgetary problems at NASA.

This grant supported our ongoing development of sensitive quasi–optical SIS mixers for the submillimeter band. The technology developed under this grant is now being applied to NASA missions, including the NASA/USRA SOFIA airborne observatory and and the ESA/NASA FIRST/Herschel space astronomy mission.

2 Summary of Technical Work
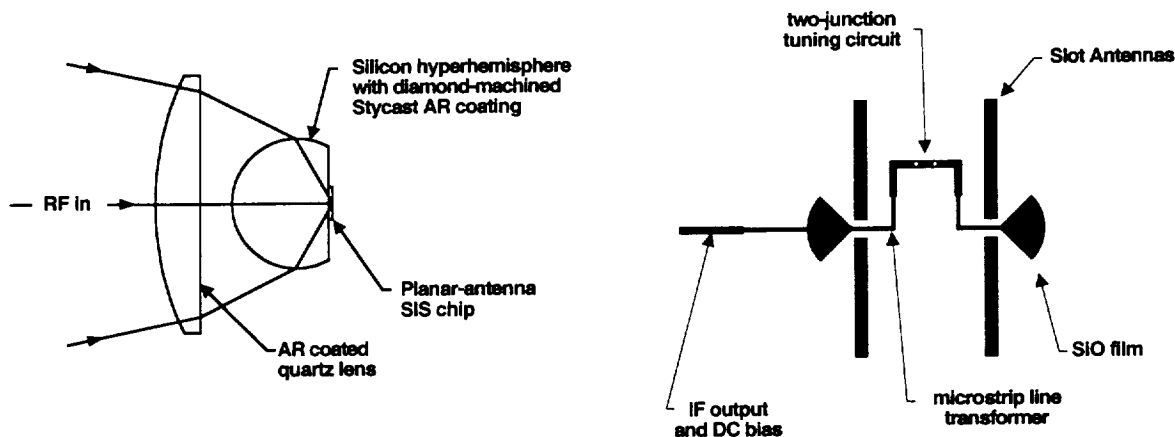
Figure 1: Our quasi–optical mixer design. *Left*: the optical configuration uses an antireflection–coated hyperhemispherical silicon lens to focus the submillimeter radiation onto the SIS chip; *Right*: the SIS chip consists of a twin slot antenna, a microstrip transformer, and a tuning circuit which uses two SIS junctions.

2.1 SIS Mixers: breakthroughs in sensitivity and bandwidth

This grant supported the development of SIS mixers for the submillimeter band (500–1200 GHz). The mixers were designed and tested at Caltech, and fabricated by the low-T_c

superconducting device group at JPL led by Dr. H. G. LeDuc. The mixers use our standard quasioptical configuration (Fig. 1). In this design, a planar twin slot antenna is lithographically fabricated along with the SIS junctions on a silicon substrate, and then this integrated "chip" is placed behind a hyperhemispherical lens which focuses the incoming radiation onto the antenna.
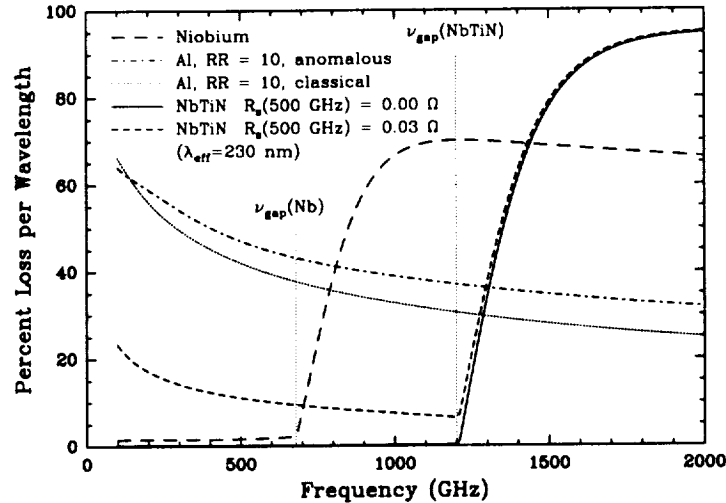

Figure 2: Calculated losses for thin–film microstrip transmission lines used in SIS mixer tuning circuits for various conductors, including NbTiN. The microstrip width is 5 μm, and the dielectric is 400 nm SiO ($\epsilon = 5.6$).

In theory, the sensitivity of SIS mixers can approach the quantum limit $T_N = h\nu/k_B$; in practice, the best results below the 700 GHz gap frequency of niobium are within a factor of 2–5 of this limit. The situation changes dramatically above 700 GHz, at which point the niobium tuning circuits become very lossy since the photon energy is large enough to break Cooper pairs ($h\nu > 2\Delta$). At these frequencies, the performance is limited by the circuit losses, even when high conductivity normal metals such as aluminum are used for the tuning circuit in place of niobium.

SIS mixers can be extended to higher frequencies by using a superconductor which has a larger gap energy and T_c. The difficulty here is finding a suitable material. The work performed under this grant demonstrated that NbTiN, which has a gap energy 1.7 times larger than niobium and a reasonably low normal–state resistivity, can provide exceptional performance in SIS circuits operating above the niobium gap frequency (700 GHz). Figure 3 shows the results for an 800 GHz mixer, which achieved a DSB noise temperature of 260 K [1]. Later improvements to the optics improved this result to around 210 K [2]. Figure 4 shows how this result compares with previous mixers: it is a factor of 2 lower noise.

Another equally significant breakthrough in SIS mixer technology was made under this
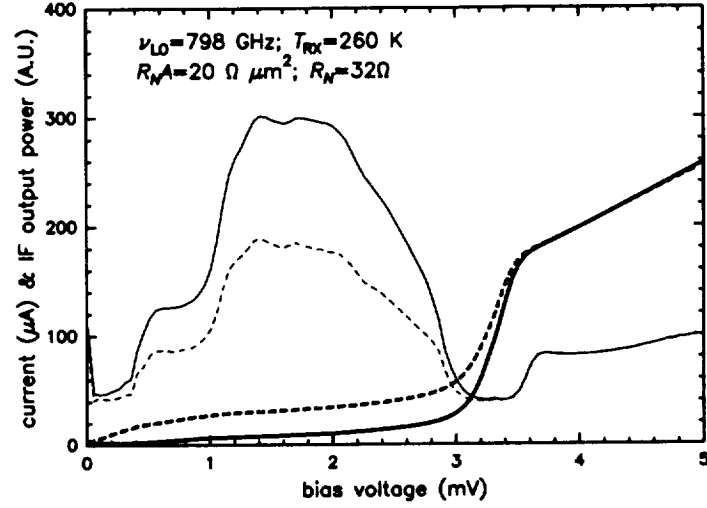
Figure 3: 800 GHz SIS mixer using NbTiN ground planes and wiring layers and Nb/AlN/NbTiN junctions. The noise temperature of 260 K is about a factor of 2 improvement over the best previous result at this frequency.
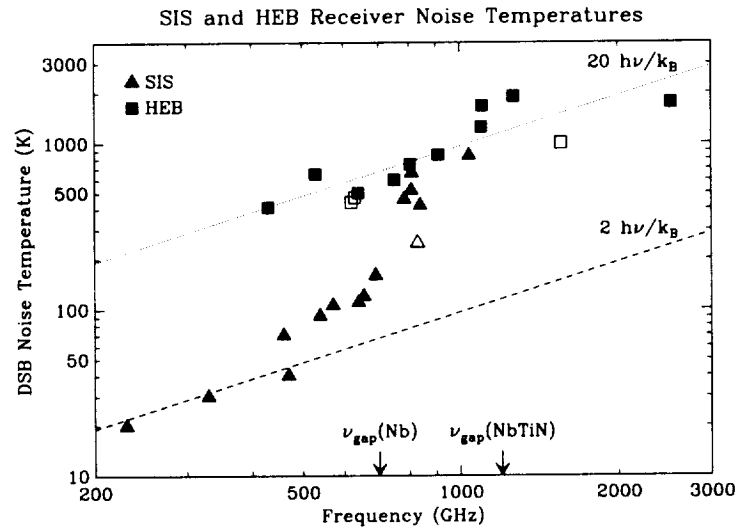

Figure 4: Selected noise temperatures obtained by various groups with SIS and HEB receivers. The open triangle near 830 GHz is our recent SIS result using NbTiN.

5

grant. This second development has to do with the material used for the tunnel barrier in the SIS junction. By replacing the standard aluminum oxide barrier with aluminum nitride (AlN), the current density of the junctions can be made at least a factor of 3 larger without a sacrifice in the leakage current. There are two reasons why this is important: first, the (fixed) tuning range of SIS mixers can now be extended from the present $\sim$ 100 GHz bandwidth to around 300 GHz, as shown in figure 5; and second, these higher current AlN junctions will be less sensitive to losses in the tuning circuits [3].
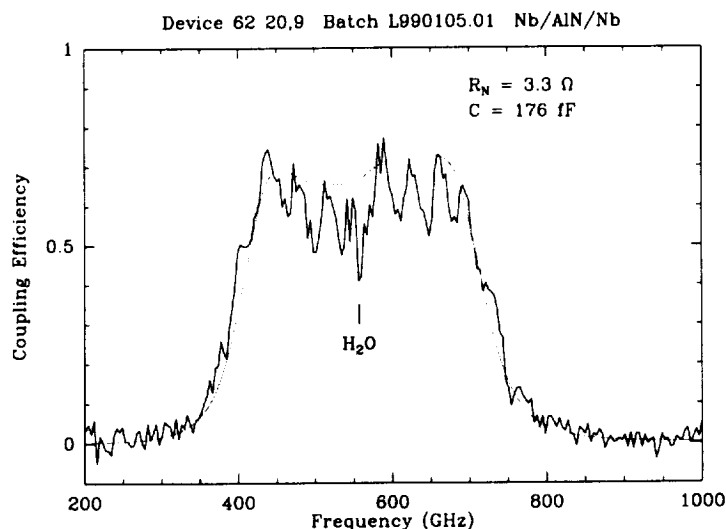
Device 62 20.9 Batch L990105.01 Nb/AlN/Nb

R_N = 3.3 Ω
C = 176 fF

H_2O

Figure 5: A measurement of the direct detection response of a twin–slot SIS mixer that uses a high current density ($\sim$ 35 kA cm^{-2}) aluminum nitride (AlN) tunnel barrier. The response band extends from 400 to 700 GHz, nearly 300 GHz wide. The heterodyne noise temperatures of such devices have also been measured, with results equivalent to devices using much lower current density (typically $\sim$ 10 kA cm^{-2}) AlOx barriers.

2.2 Dual–polarization mixers

Under the support of this grant, we also developed dual–polarization quasioptical SIS mixers. This was the thesis project of Goutam Chattopadhyay, who received his Ph.D. in Electrical Engineering from Caltech in September, 1999. Mixers for both polarizations were integrated on a single chip, using a novel dual–polarized antenna structure [4]. A 550 GHz dual polarized receiver has now been demonstrated, with a noise temperature of 120 K, and extremely good uniformity between the the two polarizations [5]. A balanced mixer based on this chip has also been demonstrated [6].

2.3 Wide IF bandwidth SIS mixers and amplifiers

At present, the instantaneous bandwidth of SIS mixers is limited to about 1 GHz, which is often insufficient, particularly for observations of external galaxies at short submillimeter wavelengths. This bandwidth limitation is mainly due to the IF amplifier. Under this grant, we have pushed to develop mixers and IF amplifers with wider bandwidths, and have demonstrated a 690 GHz mixer with 4 GHz IF bandwidth [7]. This is part of the Ph.D. thesis project for John Ward, a graduate student in physics.

2.4 SIS design software

To support our lab efforts, we have created a new new computer code called "Supermix" for analyzing and designing SIS mixers [8, 9]. Frank Rice, a graduate student is physics, had the primary responsibility for the development of this program as the first phase of his thesis research. The program, written in the C++ language, is now essentially complete and comprises around 35,000 lines of code. This code has been made available to the community, at our web site http://www.submm.caltech.edu/supermix/default.html.

3 Publications

[1] J. Kawamura, J. Chen, D. Miller, J. Kooi, J. Zmuidzinas, B. Bumble, H. G. LeDuc, and J. A. Stern, "Low-noise submillimeter-wave NbTiN superconducting tunnel junction mixers," *Appl. Phys. Lett.*, vol. 75, pp. 4013–4015, December 1999.

[2] J. Kooi, J. Kawamura, J. Chen, G. Chattopadhyay, J. Pardo, J. Zmuidzinas, T. Phillips, B. Bumble, J. Stern, and H. LeDuc, "A low noise NbTiN-based 850 GHz SIS receiver for the Caltech Submillimeter Observatory," *Int. J. IR and MM Waves*, vol. 21, no. 9, pp. 1357–1373, 2000.

[3] J. Kawamura, D. Miller, J. Chen, J. Zmuidzinas, B. Bumble, H. G. LeDuc, and J. A. Stern, "Very high current density Nb/AlN/Nb tunnel junctions for low–noise submillimeter mixers," *Appl. Phys. Lett.*, vol. 76, pp. 2119–2121, April 2000.

[4] G. Chattopadhyay and J. Zmuidzinas, "A dual–polarized slot antenna for millimeter waves," *IEEE Trans. Antennas Propagat.*, vol. 46, pp. 737–737, May 1998.

[5] G. Chattopadhyay, D. Miller, H. G. LeDuc, and J. Zmuidzinas, "A dual polarized quasi-optical SIS mixer at 550-GHz," *IEEE Trans. Microwave Theory Tech.*, vol. 48, no. 10, pp. 1680–1686, 2000.

[6] G. Chattopadhyay, F. Rice, D. Miller, H. G. LeDuc, and J. Zmuidzinas, "A 530-GHz balanced mixer," *IEEE Microwave Guided Wave Lett.*, vol. 9, pp. 467–469, November 1999.

[7] J. Ward, D. Miller, J. Zmuidzinas, P. O'Brien, H. G. LeDuc, and R. Bicknell-Tassius, "A 4–8 GHz quasi–MMIC IF amplifier for a 690 GHz SIS receiver," in *Eleventh International Symposium on Space Terahertz Technology: Symposium Proceedings*, (Ann Arbor, MI), pp. 570–581, University of Michigan, Mar. 2000.

[8] F. Rice, J. Ward, J. Zmuidzinas, and G. Chattopadhyay, "Fast harmonic balance of SIS mixers with multiple junctions and superconducting circuits," in *Tenth International Symposium on Space Terahertz Technology: Symposium Proceedings*, (Charlottesville, VA), pp. 282–297, University of Virginia, Mar. 1999.

[9] J. Ward, F. Rice, G. Chattopadhyay, and J. Zmuidzinas, "Supermix: a flexible software library for high-frequency circuit simulation, including SIS mixers and superconducting components," in *Tenth International Symposium on Space Terahertz Technology: Symposium Proceedings*, (Charlottesville, VA), pp. 268–281, University of Virginia, Mar. 1999.

[10] J. W. Kooi, J. A. Stern, G. Chattodpadhyay, H. G. LeDuc, B. Bumble, and J. Zmuidzinas, "Low–loss NbTiN films for THz SIS mixer tuning circuits," in *The Eighth International Symposium on Space Terahertz Technology: Symposium Proceedings* (R. Blundell and E. Tong, eds.), (Harvard–Smithsonian Center for Astrophysics, Cambridge, MA), pp. 310–318, 1997.

[11] J. W. Kooi, J. A. Stern, G. Chattodpadhyay, H. G. LeDuc, B. Bumble, and J. Zmuidzinas, "Low–loss NbTiN films for THz SIS mixer tuning circuits," in *Ninth International Symposium on Space Terahertz Technology: Symposium Proceedings*, (Jet Propulsion Laboratory, Pasadena, CA), pp. 283–294, Mar. 1998.

[12] J. A. Stern, B. Bumble, H. G. LeDuc, J. W. Kooi, and J. Zmuidzinas, "Fabrication and DC characterization of NbTiN based SIS mixers for use between 600 and 1200 GHz," in *Ninth International Symposium on Space Terahertz Technology: Symposium Proceedings*, (Jet Propulsion Laboratory, Pasadena, CA), pp. 305–313, Mar. 1998.

[13] J. W. Kooi, J. A. Stern, G. Chattodpadhyay, H. G. LeDuc, B. Bumble, and J. Zmuidzinas, "Low–loss NbTiN films for THz SIS mixer tuning circuits," *Int. J. IR and MM Waves*, vol. 19, pp. 373–383, 1998.

[14] J. Zmuidzinas, J. W. Kooi, J. Kawamura, G. Chattodpadhyay, J. A. Stern, B. Bumble, and H. G. LeDuc, "Development of SIS mixers for 1 THz," *Proc. SPIE*, vol. 3357, pp. 53–61, May 1998.

[15] T. de Graauw et al., "Heterodyne instrument for FIRST (HIFI): preliminary design," *Proc. SPIE*, vol. 3357, pp. 336–347, May 1998.

[16] J. Zmuidzinas, "Progress in coherent detection methods (invited)," in *The Physics and Chemistry of the Interstellar Medium* (V. Ossenkopf et al., ed.), pp. 423–430, U. Cologne, GCA–Verlag Herdecke, 1999.

[17] J. Kawamura, D. Miller, J. Kooi, J. Chen, J. Zmuidzinas, B. Bumble, H. G. LeDuc, and J. A. Stern, "Submillimeter SIS mixers using high current density Nb/AlN/Nb tunnel junctions and NbTiN films," in *Tenth International Symposium on Space Terahertz Technology: Symposium Proceedings*, (Charlottesville, VA), University of Virginia, Mar. 1999.

[18] G. Chattopadhyay, D. Miller, H. G. LeDuc, and J. Zmuidzinas, "A 550 GHz dual-polarized quasioptical SIS mixer," in *Tenth International Symposium on Space Terahertz Technology: Symposium Proceedings*, (Charlottesville, VA), pp. 130–143, University of Virginia, Mar. 1999.

[19] M. Bin, D. J. Benford, M. C. Gaidis, T. H. Büttgenbach, J. Zmuidzinas, E. Serabyn, and T. G. Phillips, "A large throughput high resolution Fourier transform spectrometer for submillimeter applications," *Int. J. IR and MM Waves*, vol. 20, pp. 383–400, 1999.

A Low–noise submillimeter–wave NbTiN superconducting tunnel junction mixers

Low-noise submillimeter-wave NbTiN superconducting tunnel junction mixers

Jonathan Kawamura,[a] Jian Chen,[b] David Miller, Jacob Kooi, and Jonas Zmuidzinas
California Institute of Technology, 320-47, Pasadena, California 91125

Bruce Bumble, Henry G. LeDuc, and Jeff A. Stern
Center for Space Microelectronics Technology, Jet Propulsion Laboratory, Pasadena, California 91108

We have developed a low-noise 850 GHz superconductor–insulator–superconductor quasiparticle mixer with NbTiN thin-film microstrip tuning circuits and hybrid Nb/AlN/NbTiN tunnel junctions. The mixer uses a quasioptical configuration with a planar twin-slot antenna feeding a two-junction tuning circuit. At 798 GHz, we measured an uncorrected double-sideband receiver noise temperature of $T_{RX}=260$ K at 4.2 K bath temperature. This mixer outperforms current Nb SIS mixers by a factor of nearly 2 near 800 GHz. The high-gap frequency and low loss at 800 GHz make NbTiN an attractive material with which to fabricate tuning circuits for SIS mixers. NbTiN mixers can potentially operate up to the gap frequency, $2\Delta/h \sim 1.2$ THz. © *1999 American Institute of Physics.* [S0003-6951(99)02651-0]

Superconductor–insulator–superconductor (SIS) quasiparticle mixers based on Nb have developed to the point that their sensitivity below the gap frequency of Nb, $2\Delta/h \approx 700$ GHz, is nearly quantum limited.[1] Quantum-limited noise performance of SIS mixers was predicted to be possible two decades ago,[2] and the development of SIS mixers has progressed steadily since then.[3,4] In terms of the single-sideband noise temperature, the quantum noise limit is $T_N = h\nu/k_B$, or $T_N/\nu \approx 48$ K THz^{-1}, and SIS receivers have reached within a factor of 10 of this fundamental limit. This level of performance has been achieved as a result of advances in the fabrication of small-area high current density Nb/AlO$_x$/Nb junctions, as well as improved mixer designs that integrate Nb superconducting tuning circuitry with the junction.

Above 700 GHz, photons have sufficient energy to break Cooper pairs in Nb, causing substantial resistive losses in tuning circuits. To produce SIS mixers for frequencies above 700 GHz, one can use a high conductivity normal metal instead of Nb in the tuning circuits.[5] Through this method, Nb SIS mixers have been extended to 1 THz; however, significant losses in the tuning circuits have prevented them from achieving near-quantum-limited performance.

Obviously, the use of superconducting materials with gap frequencies higher than that of Nb could possibly push the low-noise operation of SIS mixers above 700 GHz. The best studied material is NbN, which has a gap frequency as high as $2\Delta/h \approx 1.4$ THz in films suitable for use in mixers. However, the reported performance of NbN mixers has been somewhat disappointing: even below 700 GHz the best noise temperatures have been considerably worse than those of Nb mixers.[6–8] Though it is difficult to pinpoint the exact cause of this, two possible fundamental limitations of NbN mixers have been identified. One is excess shot noise in the junction

caused by multiple Andreév reflection tunneling in pinhole defects in NbN-based junctions.[9] A potentially more serious problem, however, is the high surface resistance of polycrystalline NbN at submillimeter wavelengths.[10]

Another possible material is NbTiN, which has a similarly high T_c, but unlike NbN, high-quality, low-resistivity films can be deposited at low substrate temperatures. The properties of NbTiN were first investigated at about the same time the first NbN films were being fabricated,[11] and there has been recent work with NbTiN films to evaluate their potential use in rf cavities for particle accelerators.[12] Our recent work[13,14] with mixers using NbTiN films has demonstrated that they can have very low loss at frequencies as high as 800 GHz, and thus may be suitable for use in mixers operating up to the gap frequency $2\Delta/h \approx 1.2$ THz. Within the past year considerable improvements have been made in our fabrication process,[15,16] and here we report on measurements made near 800 GHz on a mixer with NbTiN wiring and Nb/AlN/NbTiN junctions.

Our mixer configuration uses a quasioptical planar twin-slot antenna coupled to a two-junction tuning circuit.[17] The mixer ground plane and the microstrip wiring are made from NbTiN thin films. The mixer uses submicron hybrid Nb/AlN/NbTiN junctions. These are preferred over all-NbTiN junctions (e.g., NbTiN/MgO/NbTiN), since the subgap leakage currents are lower and current–voltage ($I-V$) characteristics are sharper. They are also preferred over Nb/AlO$_x$/Nb junctions because of their higher sum gap voltage (3.2 mV vs 2.9 mV); furthermore, the AlN tunnel barrier introduces the possibility of making junctions with extremely high current densities.[18]

The trilayer fabrication closely follows the process described previously,[15] except for two important modifications. First, we now use a Au interlayer between the NbTiN ground plane and the Nb base electrode of the junction. Our experiments comparing mixers with and without the Au layer indicate that the Au layer may be necessary to ensure a good rf contact between the NbTiN ground plane and the Nb base

[a] Electronic mail: jhk@caltech.edu
[b] On leave from the Research Institute of Electrical Communication, Tohuku University, Sendai 980-8577, Japan.
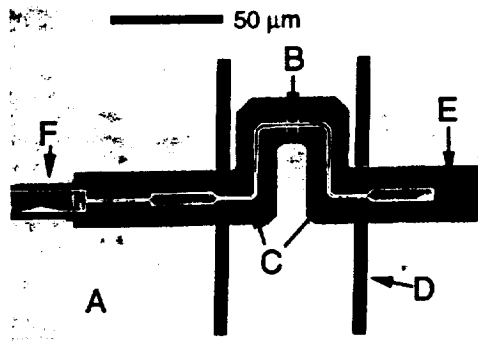
FIG. 1. A SEM image of an 850 GHz mixer. The components of the mixer labeled in the figure are as follows: (A) NbTiN ground plane; (B) two-junction tuning circuit; (C) microstrip transformers; (D) slot antenna; (E) SiO dielectric; and (F) IF output transmission line.
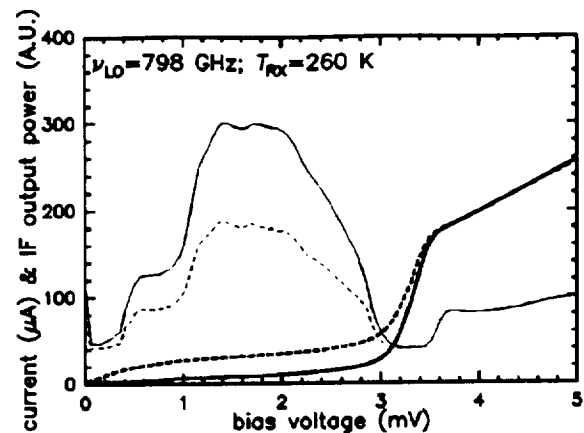
FIG. 2. Current–voltage characteristics of the 850 GHz NbTiN mixer. Shown are the $I-V$ curve traced with (dashed heavy) and without (solid heavy) LO power applied at 4.2 K bath temperature. The LO frequency is 798 GHz. The IF power in response to 295 K (solid light) and 77 K (dashed light) loads are shown as a function of voltage bias. The mixer is normally biased near 2.0 mV.

electrode. The second difference is in the plasma nitridation process for producing the AlN tunnel barrier. Previously, the rf bias for the plasma nitridation was routed through the substrate chuck. By moving the rf electrode to a different position, the system was able to produce high-quality junctions with better control and repeatability.

The fabrication of the mixer begins with the deposition of the ground plane, which is a NbTiN film deposited to a thickness of 300 nm on an unheated oxidized Si wafer. The ground plane film has $T_c \approx 15.2$ K and $\rho(20\,\mathrm{K}) \approx 75\ \mu\Omega$ cm. A thin (20 nm) blanket layer of Au is evaporated over the ground plane. On top of this, the Nb/AlN/NbTiN trilayer is fabricated. It begins with 150 nm of Nb, followed by 7 nm of Al. The AlN barrier is formed by plasma nitridation. The junction counterelectrode is 50 nm of NbTiN. The tunnel junction has a critical current density of $J_c \approx 10$ kA cm^{-1} or $R_N A \approx 20\ \Omega\ \mu\mathrm{m}^2$, and has a specific capacitance similar to AlO$_x$ for the same value of the current density.[18,19] The junctions are nominally defined to dimensions of $2.6 \times 0.25\ \mu$m using e-beam lithography employing a cross-line process.[20] The junctions are made to stretch across the width of the tuning inductor, instead of being square junctions to eliminate any spreading inductance, which considerably simplifies the mixer design calculations and reduces the rf loss in the Nb junction base electrode. Finally, after the SiO dielectric for the microstrip transmission lines is laid down, the deposition of 500-nm-thick NbTiN for the wiring layer completes the mixer. The NbTiN on SiO has a slightly lower T_c and higher resistivity, $\rho(20\,\mathrm{K}) \approx 100\ \mu\Omega$ cm. A scanning electron microscopy (SEM) image of a completed 850 GHz mixer is shown in Fig. 1.

The receiver setup is nearly identical to that used in our prior measurements of Nb SIS mixers, which gave excellent performance up to 1 THz.[5,21] The SIS mixer chip is glued to an antireflection coated Si lens. The lens/substrate combination is clamped into a copper mixer block assembly, which is mounted to the cold plate of a liquid-helium-cooled cryostat. The input beam passes through several layers of porous Teflon on the 77 K radiation shield and a high-density polyethylene lens at 4.2 K. A 25 μm mylar film serves as the vacuum window. The local oscillator (LO) is provided by a Gunn oscillator followed by two varactor multiplier stages ($\times 2 \times 3$), and is coupled to the signal beam with a 12.5 μm

Mylar beam splitter, which is about 92% transmissive near 800 GHz.

The unpumped $I-V$ curve of the 850 GHz mixer is shown in Fig. 2, which represents the two junctions connected in parallel. The junction quality is good, $R_{sg}/R_N \approx 12$, but the gap voltage is only $V_g \approx 3.2$ mV, which is considerably less than the $\sim$4.0 mV gap $(\Delta_{\mathrm{Nb}} + \Delta_{\mathrm{NbTiN}})$ we expect from this hybrid junction. This probably indicates that the NbTiN counterelectrode in the immediate vicinity of the barrier is of poorer quality.

The spectral response of this mixer was measured with a Fourier transform spectrometer (FTS), and is shown along with the predicted response in Fig. 3. The mixer model, which takes into account the slot–antenna impedance as well as the microstrip tuning circuit, agrees reasonably well with the measured response. The model calculates the surface impedance of the NbTiN films from the measured dc resistivities using the Mattis–Bardeen theory in the local limit,[22] and assumes that there are no excess losses. The effective penetration depths at 800 GHz, taking into account the finite thicknesses of the films, are calculated to be around 330 and
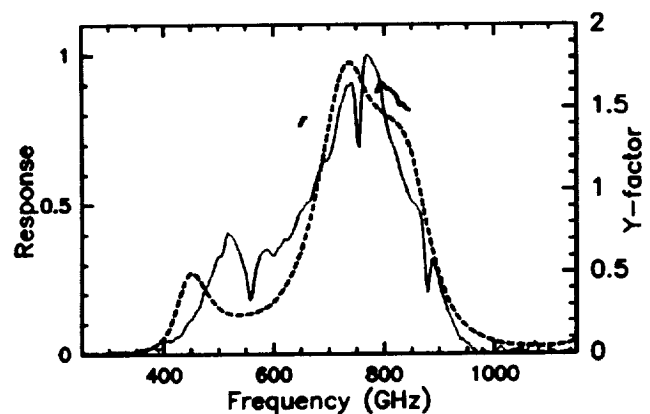
FIG. 3. Direct detection FTS measurement of the mixer's spectral response. The measured response (solid light) is plotted with a model calculation of the response (dashed heavy). These are compared to the Y factors, the heterodyne response (solid heavy). The dips in the measured spectral response are absorption lines.
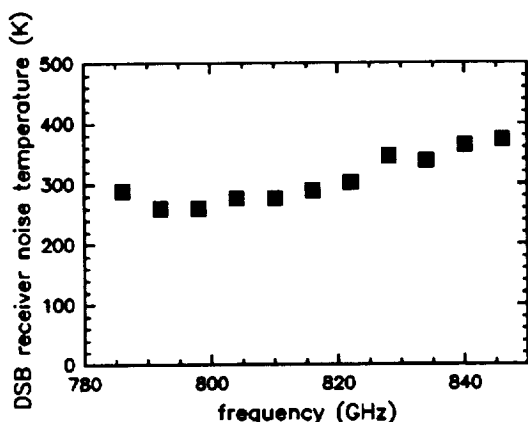
FIG. 4. Receiver noise temperature as a function of frequency across the operating bandwidth of the LO source. These are the same data as presented in Fig. 3.

310 nm for the ground plane and wiring, respectively. The specific capacitance of the AlN–barrier junctions was assumed to be 85 fF μm^{-2}, as was measured using Nb tuning circuits.[18] The frequency width of the measured response indicates that the NbTiN surface resistance has an upper limit of roughly $R_S < 0.1\,\Omega$ near 800 GHz, which is less than the surface resistance of a polycrystalline NbN film.[10] In our mixer, an excess surface resistance of $0.1\,\Omega$ (in the wiring layer only) would translate to an additional ~ 0.5 dB of conversion loss.

Heterodyne noise measurements of the mixer are summarized in Fig. 4. For these measurements, the standard Y-factor technique was used, and the equivalent load temperatures were computed using the Callen–Welton formula $T_{input} = (h\nu/2k)\coth(h\nu/2kT_{load})$. No corrections were applied; the raw Y factors are plotted with the spectral response curve in Fig. 3. The receiver noise temperature follows the spectral profile measured by the FTS. The best double sideband receiver noise temperature was $T_{RX} = 260$ K at a LO frequency of 798 GHz, as shown in Fig. 2. For best noise performance, the mixer should be biased near 2 mV. The first Shapiro step occurs at $V \approx 1.65$ mV, but has been successfully suppressed using a magnetic field. The photon-assisted tunneling step should start at $V = V_{gap} - h\nu/e \approx 0.1$ mV, and the pumped curve gives an indication of this.

From the heterodyne measurements, we can estimate the mixer conversion loss and compare it to a theoretical value, and thereby obtain an upper limit to the loss in the tuning circuit. Using the shot-noise technique[23] to calibrate the IF system, we estimate that the mixer conversion loss is $L \approx 8.5$ dB (single sideband). Applying Tucker's theory[3] in the three-port approximation to our mixer, we calculate that the intrinsic mixer conversion loss is 7.0 dB. Together with 0.7 dB loss from the vacuum window, 0.4 dB loss from the beam splitter, and about 0.5 dB loss in the cold optics, the total predicted receiver conversion loss is $L \approx 8.6$ dB, which

closely matches the measured value. This suggests that the loss of the NbTiN tuning circuit has an upper limit comparable to the uncertainty of the measurements (~ 1 dB). This is in agreement with the upper limit on the loss established by modeling the spectral response of the receiver.

Note added in proof: Recent measurements with improved optics have yielded $T_{RX} = 205$ K (DSB) at 798 GHz.

[1] J. Carlstrom and J. Zmuidzinas, in *Review of Radio Science 1993–1996*, edited by W. R. Stone (Oxford University Press, Oxford, 1996), pp. 839–882.
[2] J. R. Tucker, IEEE J. Quantum Electron. **15**, 1234 (1979).
[3] J. R. Tucker and M. J. Feldman, Rev. Mod. Phys. **57**, 1055 (1985).
[4] R. Blundell and C.-Y. E. Tong, Proc. IEEE **80**, 1702 (1992).
[5] M. Bin, M. C. Gaidis, J. Zmuidzinas, T. G. Phillips, and H. G. LeDuc, Appl. Phys. Lett. **68**, 1714 (1996).
[6] W. R. McGrath, J. A. Stern, H. H. S. Javadi, S. R. Cypher, B. D. Hunt, and H. G. LeDuc, IEEE Trans. Magn. **27**, 2650 (1991).
[7] Y. Uzawa, Z. Wang, and A. Kawakami, IEEE Trans. Appl. Supercond. **7**, 2574 (1997).
[8] A. Karpov, B. Plathner, and J. Blondel, IEEE Trans. Appl. Supercond. **7**, 1077 (1997).
[9] P. Dieleman, H. G. Bukkems, T. M. Klapwijk, M. Schicke, and K. H. Gundlach, Phys. Rev. Lett. **79**, 3486 (1997).
[10] S. Kohjiro, S. Kiryu, and A. Shoji, IEEE Trans. Appl. Supercond. **3**, 1965 (1993).
[11] J. R. Gavaler, J. K. Hulm, M. A. Janocko, and C. K. Jones, J. Vac. Sci. Technol. **6**, 177 (1968).
[12] R. D. Leo, A. Nigro, G. Nobile, and R. Vaglio, J. Low Temp. Phys. **78**, 41 (1990).
[13] J. W. Kooi, J. A. Stern, G. Chattopadhyay, H. G. LeDuc, B. Bumble, and J. Zmuidzinas, Int. J. Infrared Millim. Waves **19**, 373 (1998).
[14] J. Zmuidzinas, J. Kooi, J. Kawamura, G. Chattopadhyay, B. Bumble, H. G. LeDuc, and J. A. Stern, Proc. SPIE **3357**, 53 (1998).
[15] B. Bumble, H. G. LeDuc, and J. A. Stern, in *Proceedings of the 9th International Symposium on Space THz Technology*, edited by W. R. McGrath (Jet Propulsion Laboratory, Pasadena, CA, 1998), pp. 295–304.
[16] J. A. Stern, B. Bumble, H. G. LeDuc, J. W. Kooi, and J. Zmuidzinas, in *Proceedings of the 9th International Symposium on Space THz Technology*, edited by W. R. McGrath (Jet Propulsion Laboratory, Pasadena, CA 1998), pp. 305–313.
[17] J. Zmuidzinas, H. G. LeDuc, J. A. Stern, and S. R. Cypher, IEEE Trans. Microwave Theory Tech. **42**, 698 (1994).
[18] J. Kawamura, D. Miller, J. Chen, J. Zmuidzinas, B. Bumble, H. G. LeDuc, and J. A. Stern (unpublished).
[19] A. W. Kleinsasser, W. H. Mallison, and R. E. Miller, IEEE Trans. Appl. Supercond. **5**, 2318 (1995).
[20] M. Aoyagi, S. Kosaka, F. Shinoki, and S. Takada, in *Extended Abstracts of the 1987 International Superconducting Electronics Conference* (ISEC, Tokyo, 1987), pp. 222–225.
[21] M. C. Gaidis, H. G. LeDuc, M. Bin, D. Miller, J. A. Stern, and J. Zmuidzinas, IEEE Trans. Microwave Theory Tech. **44**, 1130 (1996).
[22] D. C. Mattis and J. Bardeen, Phys. Rev. **111**, 412 (1979).
[23] D. P. Woody, R. E. Miller, and M. J. Wengler, IEEE Trans. Microwave Theory Tech. **33**, 90 (1985).

B Very high–current–density Nb/AlN/Nb tunnel junctions for low–noise submillimeter mixers

Very high-current-density Nb/AlN/Nb tunnel junctions for low-noise submillimeter mixers

Jonathan Kawamura,[a] David Miller, Jian Chen,[b] and Jonas Zmuidzinas
California Institute of Technology, 320-47, Pasadena, California 91125

Bruce Bumble, Henry G. LeDuc, and Jeff A. Stern
Center for Space Microelectronics Technology, Jet Propulsion Laboratory, Pasadena, California 91108

We have fabricated and tested submillimeter-wave superconductor–insulator–superconductor (SIS) mixers using very high-current-density Nb/AlN/Nb tunnel junctions ($J_c \approx 30\,\mathrm{kA\,cm^{-2}}$). The junctions have low-resistance-area products ($R_N A \approx 5.6\,\Omega\,\mu\mathrm{m}^2$), good subgap-to-normal resistance ratios $R_{sg}/R_N \approx 10$, and good run-to-run reproducibility. From Fourier transform spectrometer measurements, we infer that $\omega R_N C = 1$ at 270 GHz. This is a factor of 2.5 improvement over what is generally available with Nb/AlOx/Nb junctions suitable for low-noise mixers. The AlN-barrier junctions are indeed capable of low-noise operation: we measure an uncorrected double-sideband receiver noise temperature of $T_{RX} = 110\,\mathrm{K}$ at 533 GHz for an unoptimized device. In addition to providing wider bandwidth operation at lower frequencies, the AlN-barrier junctions will considerably improve the performance of THz SIS mixers by reducing rf loss in the tuning circuits. © 2000 American Institute of Physics. [S0003-6951(00)04915-9]

Niobium-based superconductor–insulator–superconductor (SIS) tunnel junction mixers have now achieved near-quantum-limited noise performance in the near-millimeter bands,[1] as was predicted to be possible theoretically.[2,3] This success relies heavily on advances in the technology for fabricating high-quality small-area niobium junctions with aluminum oxide barriers (Nb/AlOx/Nb), along with integrated Nb thin-film superconducting tuning circuits. The tuning circuits are necessary to overcome the frequency response limitation imposed by the finite resistance–capacitance ($R_N C$) product of SIS junctions: the 3 dB roll off in the frequency response ($\omega R_N C = 1$) of an untuned Nb/AlOx/Nb junction occurs at approximately 100 GHz. Here, R_N is the junction normal resistance and C is its capacitance.

An inductive tuning circuit with inductance L allows the center frequency $\nu_0 = \omega_0/2\pi$ of the response to be chosen arbitrarily, according to the usual condition $\omega_0^2 L C = 1$, with a response bandwidth that is limited by the $R_N C$ product. Either a series or parallel inductance can be used, and is most often provided by a section of superconducting microstrip transmission line. In practice, rf losses in the tuning circuit seriously limit the performance at higher frequencies. Tuning circuits made from Nb become ineffective above 700 GHz, due to the onset of large Ohmic losses (surface resistance) above the superconducting energy-gap frequency $\nu_{gap} = 2\Delta/h$. At present, one of the main goals of SIS mixer development, driven by the needs of airborne and space-based astronomy projects, is to extend their low-noise performance to frequencies above 1 THz.

For operation above 700 GHz, a high conductivity normal metal (e.g., Al) can be used in place of niobium for the tuning circuit.[4] Another possibility is to use a low-loss superconductor with a larger energy gap, such as NbTiN.[5] In either approach, the resulting resonant circuit requires a large quality factor ($Q \sim 10$ at 1 THz) for ideal performance and is, therefore, quite sensitive to Ohmic loss. For instance, in mixers which use normal metal tuning circuits, much of the rf power is still dissipated in the tuning circuit, and only a small fraction (~20%) of the signal is absorbed (detected) by the tunnel junction. High-frequency Ohmic loss is an important issue even for superconducting films (e.g., NbTiN), since the loss is often a sensitive function of film quality, composition, and microstructure, and can be difficult to control. In many SIS mixer designs, superconducting microstrip lines are also used for the impedance transformers which match the circuit to the rf feed, which can either be a planar antenna structure or a waveguide-to-microstrip transition. Although there may be losses in these transformers as well, the mixer's overall performance depends most critically on the inductive circuit which tunes out the junction capacitance, due to its high-Q requirement.

Thus, an important parallel strategy is to reduce the junction $R_N C$ product, so that the Q required for the tuning circuit is reduced and the mixer performance is less sensitive to losses. The $R_N C$ product is independent of junction area, but depends critically on the thickness of the tunnel barrier. Because the tunneling resistance decreases exponentially as the barrier thickness t is reduced, while the capacitance should increase only as $1/t$, thinner tunnel barriers are needed to reduce the $R_N C$ product. Two parameters are commonly used to characterize the tunnel barrier: the Josephson critical current density J_c and the resistance-area product $R_N A$. However, there is a serious practical difficulty associated with increasing the current density (reducing $R_N A$): at some point, the junction quality degrades rapidly.

An important figure of merit for SIS junctions used in low-noise mixer applications is the subgap-to-normal resistance ratio R_{sg}/R_N, which is a measure of the junction leak-

[a] Electronic mail: jhk@caltech.edu
[b] On leave from the Research Institute of Electrical Communication, Tohoku University, Sendai 980-8577, Japan.

age current. This quantity controls the conversion efficiency and noise of the mixer.[3] For Nb/AlOx/Nb junctions, the subgap-to-normal resistance ratio degrades rapidly for current densities much higher than 10 kA cm^{-2}.[6] This corresponds to a resistance-area product of $R_N A \approx 20\,\Omega\,\mu$m^2. There is good evidence[7] that the quality degradation of Nb/AlOx/Nb tunnel junctions is caused by pinhole defects in the barrier. For $R_N A \approx 20\,\Omega\,\mu$m^2, the junction specific capacitance is $C_s \approx 85$ fF μm^{-2}; combining these quantities, one obtains the roll-off frequency $(2\pi R_N C)^{-1} \approx 100$ GHz quoted above.

It is possible to fabricate high-quality junctions with higher current densities by using AlN as the barrier material.[8] We have recently fabricated Nb/AlN/Nb junctions with current densities as high as $J_c \approx 50$ kA cm^{-2}. The high-current-density AlN junctions have also been incorporated into submillimeter mixer circuits, using an existing design. This design, which was optimized for Nb/AlOx/Nb junctions with $J_c \approx 10$ kA cm^{-1}, has a well-understood behavior and has demonstrated excellent performance.[9] We assumed that this approach would be adequate, since the specific capacitance of AlN junctions was previously estimated to be roughly similar to that of AlOx junctions,[8] and since the capacitance should only be a slow function of current density.

The fabrication of the mixers largely followed the steps used to make the previous devices, with one exception. Instead of following the Al deposition by oxidation to form an oxide barrier, an AlN barrier was formed by plasma nitridation.[10] In this process, 7 nm of Al is sputtered on a Nb ground plane, and the nitride barrier is formed by exposing it to a pure nitrogen plasma. The ground plane and wiring layer Nb film are 170 and 300 nm thick, respectively. The junctions are square and have a nominal area in the range $A = 1.2$–$2.25\,\mu$m^2. The target current density is $J_c \approx 30$ kA cm^{-2}, which yields junctions with $R_N A = 5.6\,\Omega\,\mu$m^2. We obtain good subgap-to-normal resistance ratios, $R_{sg}/R_N \approx 10$. The current–voltage characteristics of one of the mixers are shown in Fig. 1. A batch of mixers with lower current density was also fabricated, with $R_N A = 20\,\Omega\,\mu$m^2. These mixers have very similar R_{sg}/R_N ratios as the high-current-density devices, which allow the mixer characteristics to be directly compared.

The mixer configuration we use is a quasioptical planar twin-slot antenna coupled to a two-junction tuning circuit.[11] The completed mixer chip is attached to an antireflection-coated hyperhemispherical Si lens. The lens and substrate are fitted into a copper mixer block assembly, which is mounted on a liquid-helium-cooled cold plate. The input beam passes through a high-density polyethylene lens at 4.2 K and several layers of infrared filtering provided by porous Teflon on the 77 K radiation shield. The vacuum window is a 25-μm-thick mylar film. The local oscillator is coupled to the input beam with a 12-μm-thick mylar beam splitter at room temperature. The intermediate frequency is centered at 1.5 GHz and the first-stage amplification is provided by a high-electron-mobility transistor amplifier with an input noise of $T_{if} \approx 5$ K.

The spectral response of 650 GHz mixers with both high and normal current densities was measured with Fourier

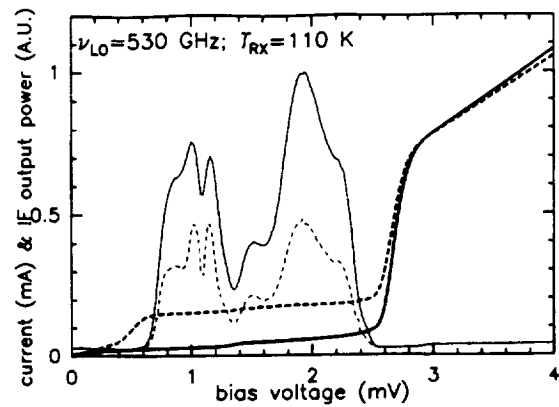FIG. 1. Current–voltage $(I-V)$ characteristics of a high-current-density 550 GHz mixer. The bath temperature is 4.2 K. Shown are the $I-V$ characteristics traced with (dashed heavy) and without (solid heavy) local-oscillator power applied. The LO frequency is 533 GHz, and the photon step begins at $V \approx 0.6$ mV. The if power in response to 295 K (solid light) and 77 K (dashed light) loads is shown as a function of voltage bias. The bumps in the if power response near $V \approx 1.2$ mV reflect insufficient supression of Josephson currents. The mixer is normally biased near 2.0 mV for best performance. For this measurement, a 12.5 μm Mylar beam splitter was used to couple the optimum amount of LO power to the mixer, and $T_{RX}=110$ K.

transform spectrometer (FTS), and the results are shown in Fig. 2. The difference between the two mixers is quite dramatic, as the response of the mixer with higher current density spans nearly an octave. FTS measurements were made on a number of other devices, and are summarized in Fig. 3. The response curves were fitted with a mixer model, which takes into account the frequency-dependent impedance of the slot antenna and the behavior of the tuning circuit. The surface impedance of the niobium films used in the microstrip transmission lines was calculated using Mattis–Bardeen theory in the local limit.[12] The model response was multiplied by the antenna main-beam efficiency to simulate the mixer's coupling to the FTS. In general, the main-beam efficiency varies only slowly near the center frequency but decreases rapidly at high frequencies due to the onset of large sidelobes in the antenna pattern.

The junction capacitance and normal-state resistivity of the niobium films are the main physical parameters that are derived by adjusting the mixer model to fit the measure-
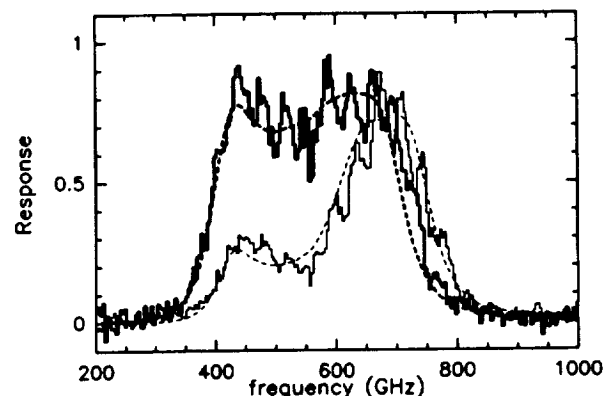

FIG. 2. Direct detection FTS response of Nb/AlN/Nb mixers with $J_c \sim 30$ kA cm^{-2} (heavy) and $J_c \sim 10$ kA cm^{-2} (light) current densities. The measured receiver responses are indicated by histograms, and the model fits to these are the dashed curves. For the high-current-density mixer, we infer $\omega RC = 1$ at 270 GHz, whereas for the low current density mixer, $\omega RC = 1$ at 110 GHz.

Appl. Phys. Lett., Vol. 76, No. 15, 10 April 2000
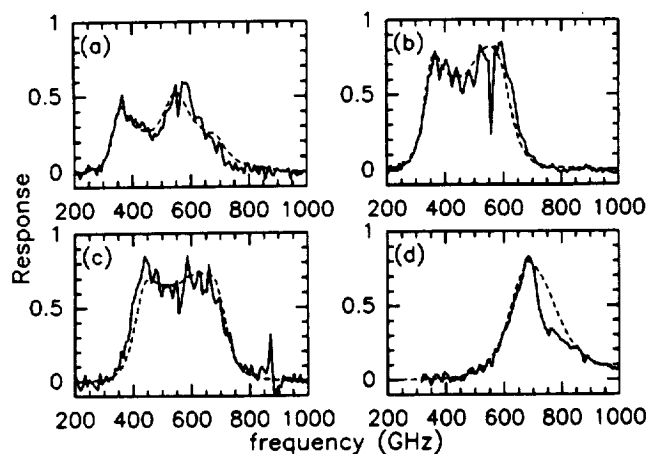
Kawamura et al.   2121

FIG. 3. Direct detection FTS response plotted with mixer model calculations for a number of different mixers with very high-current-density junctions: (a) a 550 GHz mixer with junction area $A = 0.8\ \mu m^2$; (b) 550 GHz mixer, $A = 1.3\ \mu m^2$; (c) 650 GHz mixer, $A = 1.7\ \mu m^2$; and (d) 750 GHz mixer, $A = 1.0\ \mu m^2$.

ments. In our simulations, the normal-state resistivity ρ_n is only used as a scaling parameter for the Mattis–Bardeen complex conductivity, so adjusting ρ_n is equivalent to changing the penetration depth. The FTS curves are quite well described by the model, and provide tight constraints on the physical parameters. The junction specific capacitance C_s can be calculated by dividing the junction capacitance used in the mixer model by the junction area. The junction areas are inferred from the junction resistance R_N, by assuming that the resistance-area product $R_N A$ is constant across the wafer and is given by the value deduced from a set of test junctions with a wide range of junction areas.

From the mixer models, we find $\rho = 4\ \mu\Omega$ cm for the Nb film normal-state resistivity and $C_s = 105\ fF\ \mu m^{-2}$ for the specific capacitance of the high-current-density junctions. The specific capacitance for the low-J_c AlN junctions is found to be $C_s = 85\ fF\ \mu m^{-2}$, which is very similar to that of AlOx barrier junctions with the same current density. The value for the normal-state resistivity is consistent with that actually measured for similar films. By combining the junction capacitance determined by modeling with the junction resistance (trivially determined from dc measurements), we find that $\omega R_N C = 1$ at 270 GHz for the high-current-density mixers. For comparison, for the low-current-density mixers, we find $\omega R_N C = 1$ at 110 GHz, which is close to that attained with Nb/AlOx/Nb junctions. Thus, the $R_N C$ product of the high-current-density junction mixers represents an improvement by a factor ~2.5 over what is presently attainable from Nb/AlOx/Nb junctions. Note that our determination of the $R_N C$ product does not depend on accurate knowledge of the junction area; the area is needed only to calculate the specific capacitance.

Finally, the sensitivity of a high-current-density mixer was measured using the standard Y-factor technique. For a

mixer designed for operation near 550 GHz, we measured a double-sideband receiver noise temperature of $T_{RX} = 110$ K at 530 GHz, with no corrections applied. The spectral response of this mixer is shown in Fig. 3(b), and its current–voltage characteristics and intermediate frequency (if) output power in response to hot (295 K) and cold (77 K) loads are shown in Fig. 1. We stress that the mixer circuit design was optimized for a junction with $R_N A \approx 20\ \Omega\ \mu m^2$, so the coupling is not optimal at either the if or the rf. Regardless, the performance at 530 GHz is still excellent and is comparable to our best results with this mixer design and receiver configuration when employing lower-J_c Nb/AlOx/Nb mixers. This measurement confirms that the high-current-density junctions used in our study are capable of low-noise mixing.

The use of high-current-density SIS mixers should greatly advance the development of low-noise terahertz mixers. Generally, it should greatly relax the requirements on the losses in tuning circuits. In particular, it should be possible to improve the noise performance of a mixer that uses a normal-metal tuning circuit by a factor of at least 2 near 1 THz. Finally, the reduction in the $R_N C$ product naturally allows the construction of mixers with very large input bandwidths. This is important especially at higher frequencies where the wider bandwidth allows a given frequency range to be covered with fewer mixers, resulting in simplified instrument designs.

[1] J. Carlstrom and J. Zmuidzinas, in Review of Radio Science 1993–1996, edited by W. R. Stone (Oxford University Press, Oxford, 1996), pp. 839–882.
[2] J. R. Tucker, IEEE J. Quantum Electron. 15, 1234 (1979).
[3] J. R. Tucker and M. J. Feldman, Rev. Mod. Phys. 57, 1055 (1985).
[4] M. Bin, M. C. Gaidis, J. Zmuidzinas, T. G. Phillips, and H. G. LeDuc, Appl. Phys. Lett. 68, 1714 (1996).
[5] J. Kawamura, J. Chen, D. Miller, J. Kooi, J. Zmuidzinas, B. Bumble, H. G. LeDuc, and J. A. Stern, Appl. Phys. Lett. 75, 4013 (1999).
[6] R. E. Miller, W. H. Mallison, A. W. Kleinsasser, K. A. Delin, and E. M. Macedo, Appl. Phys. Lett. 63, 1423 (1993).
[7] A. W. Kleinsasser, R. E. Miller, W. H. Mallison, and G. B. Arnold, Phys. Rev. Lett. 72, 1738 (1994).
[8] A. W. Kleinsasser, W. H. Mallison, and R. E. Miller, IEEE Trans. Appl. Supercond. 5, 2318 (1995).
[9] M. C. Gaidis, H. G. LeDuc, M. Bin, D. Miller, J. A. Stern, and J. Zmuidzinas, IEEE Trans. Microwave Theory Tech. 44, 1130 (1996).
[10] B. Bumble, H. G. LeDuc, and J. A. Stern, in Proceedings of the 9th International Symposium on Space THz Technology, edited by W. R. McGrath (Jet Propulsion Laboratory, Pasadena, CA, 1998), pp. 295–304.
[11] J. Zmuidzinas, H. G. LeDuc, J. A. Stern, and S. R. Cypher, IEEE Trans. Microwave Theory Tech. 42, 698 (1994).
[12] D. C. Mattis and J. Bardeen, Phys. Rev. 111, 412 (1958).

C A 530 GHz Balanced Mixer

A 530-GHz Balanced Mixer

Goutam Chattopadhyay, *Student Member, IEEE*, Frank Rice, David Miller,
Henry G. LeDuc, and Jonas Zmuidzinas, *Member, IEEE*

Abstract— We report on the design and performance of a
530-GHz balanced SIS mixer, the first balanced mixer in this
frequency range. This quasi-optical balanced mixer utilizes a
cross-slot antenna on a hyperhemispherical substrate lens with
eight superconductor–insulator–superconductor (SIS) junctions
and a 180° lumped element IF hybrid circuit. The local oscil-
lator (LO) and the radio frequency (RF) signal, orthogonal in
polarization to each other, are coupled to the mixer using a wire-
grid polarizer. The noise performance of the mixer is excellent,
giving an uncorrected receiver noise temperature of 105 K (DSB)
at 528 GHz.

Index Terms— Balanced mixer, low noise, superconductor–
insulator–superconductor (SIS) junctions.

I. INTRODUCTION

BALANCED mixers suppress local oscillator (LO) ampli-
tude modulation (AM) noise, have better power handling
capabilities, and reject certain spurious responses and spurious
signals [1]. At millimeter and submillimeter wavelengths,
single-ended mixers are almost always used, and LO injection
is usually accomplished using an optical beamsplitter or a
waveguide coupler. However, due to the low available LO
power in this frequency range, the coupling often must be
fairly large, −10 dB or greater. Since the LO is usually at
room temperature, this results in 30 K or more of thermal
noise being injected into the receiver along with the LO.
This can be a rather significant contribution to the total
receiver noise temperature; modern superconductor insulator
superconductor (SIS) receivers can have noise temperatures
well below 100 K. In contrast, balanced mixers are capable
of rejecting the thermal noise incident at the LO port. In
addition, balanced mixers make use of *all* of the available
LO power, whereas single-ended mixers with beamsplitters
or couplers waste ≥90% of the LO power. These advantages
have also been noted by Kerr *et al.* [2]. However, no balanced
mixer results have been reported to date at submillimeter
wavelengths. Stephan *et al.* proposed the first quasioptical
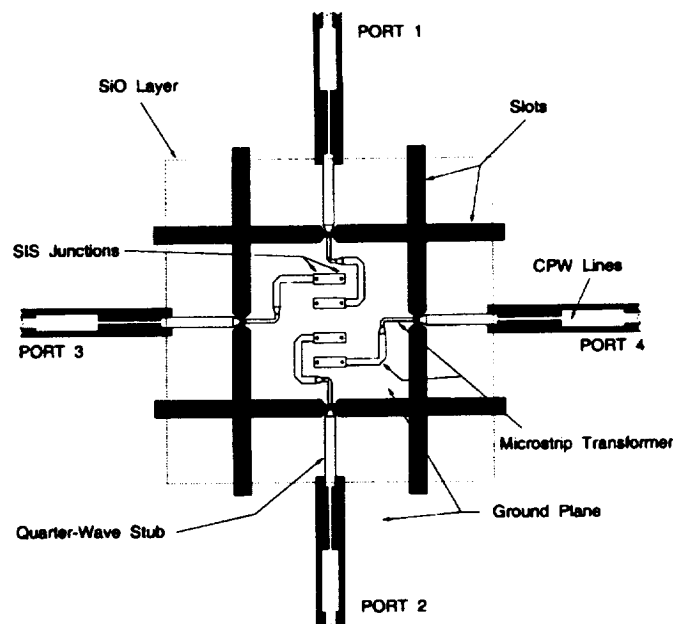balanced mixer at 90 GHz [3], and Tong *et al.* proposed a

Fig. 1. Details of the mixer chip layout. CPW lines carry IF outputs which
are combined to get the balanced output signal.

magic tee balanced mixer which potentially could be used at
millimeter wavelengths [4]. Kerr *et al.* reported the design of
a waveguide balanced mixer for 200–300 GHz [2], but no
experimental results were given.

II. MIXER CONFIGURATION AND DESIGN

We have designed and fabricated a quasi-optical balanced
superconductor–insulator–superconductor (SIS) mixer at
530 GHz. The mixer utilizes a cross-slot antenna on a
hyperhemispherical substrate lens which has symmetric E-
and H-plane beams, low impedance, wide bandwidth, low
cross polarization, and high coupling efficiency [5]. Instead of
designing a new chip for this mixer, we used the dual-polarized
SIS mixer chip described by Chattopadhyay *et al.* [6]. A layout
of the mixer chip is shown in Fig. 1. This mixer chip has
four antenna ports with a two junction SIS circuit connected
to each of the ports. The radiation received by the cross-slot
antenna is coupled into the SIS junctions with superconducting
microstrip lines. The two-section quarter-wave microstrip
transformer allows a good impedance match between the
antenna ($\approx 30\ \Omega$) and the tunnel junctions ($R_n/2 \approx 7\ \Omega$).
Balanced mixer operation is achieved by coupling the LO
and the RF signals in two orthogonal polarizations using a
wire-grid polarizer and combining the IF outputs using a 180°
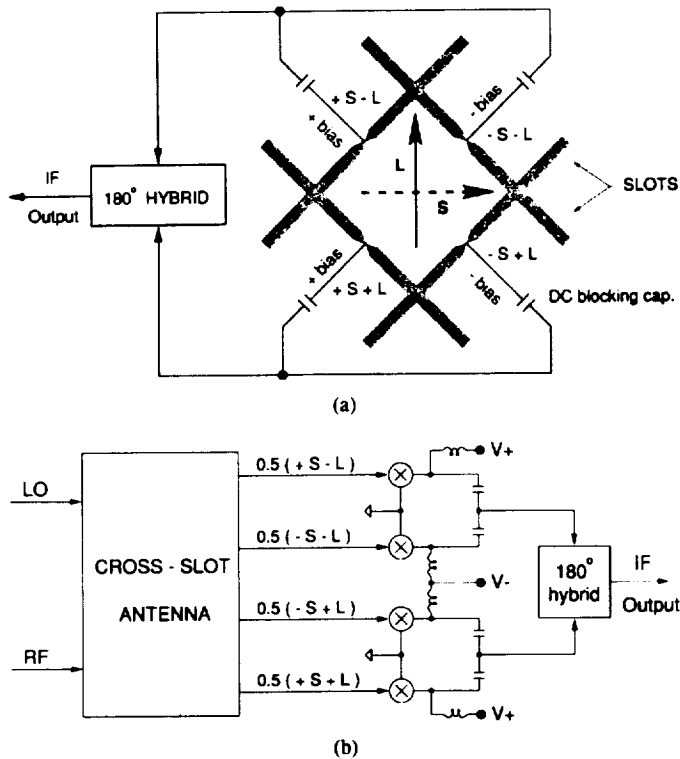hybrid circuit.

(a)

(b)

Fig. 2. Balanced mixer configuration using the dual-polarized mixer chip. (a) Cross-slot antenna with different signals and circuits. LO and RF signals (denoted as L and S, respectively) with the phases are shown at the four antenna ports. (b) Corresponding functional diagram.
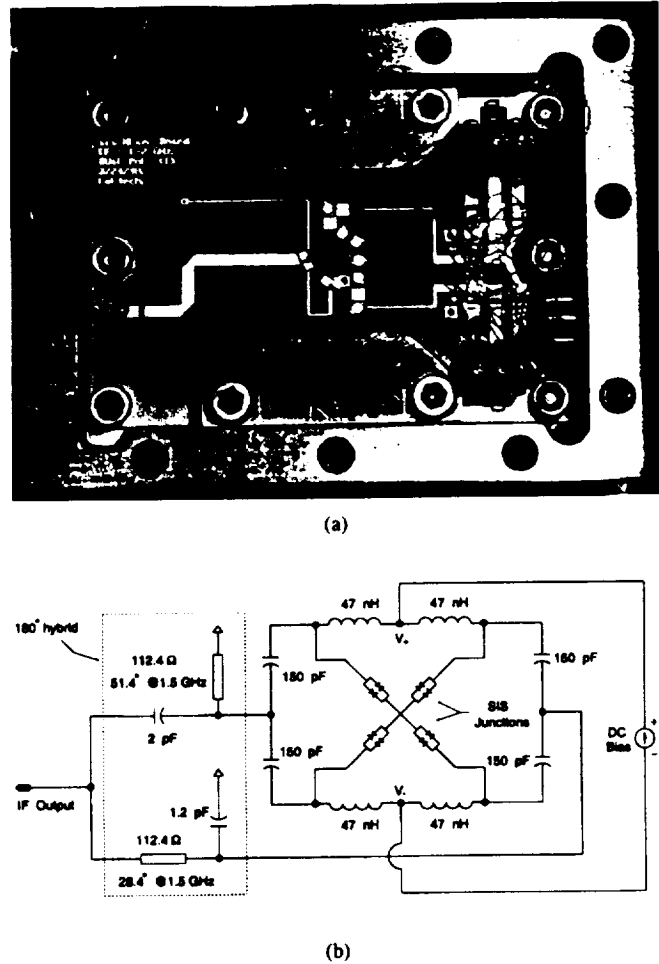

(a)

(b)

Fig. 3. Biasing and IF circuit details. (a) Mixer block with IF circuit board. The IF output is taken out through the SMA connector shown on the left and the bias comes in through the connector on the right. (b) Details of the IF and dc bias circuits.

Our implementation of a balanced mixer using the cross-slot antenna is shown in Fig. 2. In Fig. 2(a), the LO and RF signals are denoted by L and S, respectively, and have orthogonal polarizations, as shown. Also shown in the figure are the phases of the LO and RF signals at the four ports of the cross-slot antenna ($+S - L$, $+S + L$ etc.). The four IF outputs, as shown, are dc blocked and combined in a 180° hybrid circuit. Fig. 2(b) shows the corresponding functional diagram for the balanced mixer. It is to be noted that due to the mandatory series biasing of the mixers, the currents in the ports which are positively biased will be 180° out of phase compared to the currents in the mixers which are negatively biased [6]. This is taken into account in the functional diagram in Fig. 2(b).

The assembled balanced mixer circuit is shown in the Fig. 3(a). The bias for the SIS junctions come in through a connector from the right side and the IF output comes out of the mixer block on the left through a SMA connector as shown. The mixer chip is placed on an antireflection coated silicon hyperhemispherical lens, and the 180° IF hybrid circuit is realized using lumped capacitors and microstrip transmission lines as in [6]. The details of the IF and dc circuits are shown in Fig. 3(b).

III. MEASUREMENT AND RESULTS

The receiver response as a function of frequency was measured with an fourier transform spectroscopy (FTS) system using the mixer as a direct detector. Fig. 4 shows the FTS response for the mixer chip along with the simulation results

obtained from the "Pcircuit" program [7]. The FTS response agrees reasonably well with the simulation results, and the peak response was found at 528 GHz. Since the RF junction impedances in heterodyne and in direct detection operation typically differ by less than 10%, the direct FTS measurements can be expected to give relatively accurate indication of the device frequency dependence in heterodyne mode [8], [9], which means that the noise temperature for this mixer will follow the FTS curve and the best noise temperature would be around 528 GHz. As can be seen in Fig. 4, the measured FTS response has a narrower bandwidth than predicted by our design simulation. We believe that this discrepancy can largely be attributed to differences in the device parameters assumed for the design versus those actually achieved in fabrication, particularly the properties of the microstrip dielectric layer.

The noise temperature measurement setup for the balanced mixer is shown in Fig. 5. The wire-grid polarizer reflects the vertically polarized LO signal and passes the horizontally polarized RF signal. The combined LO and RF signals, after passing through the optics, is incident on to the mixer inside the cryostat. The cross-slot antenna is oriented as shown in Fig. 2(a). The IF output is amplified by a 1.0–2.0 GHz cooled HEMT low-noise amplifier (LNA) with a measured
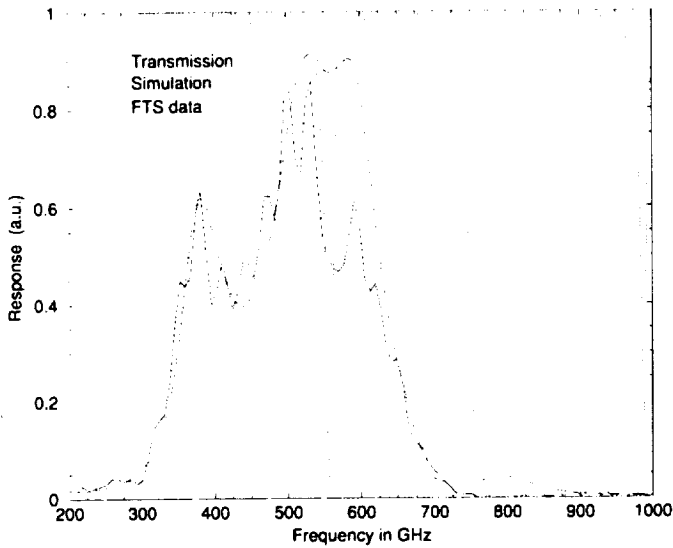
Fig. 4. FTS response. Solid line is the measured response, and the dashed line is the simulation result. The dotted line shows the transmission for the instrument.
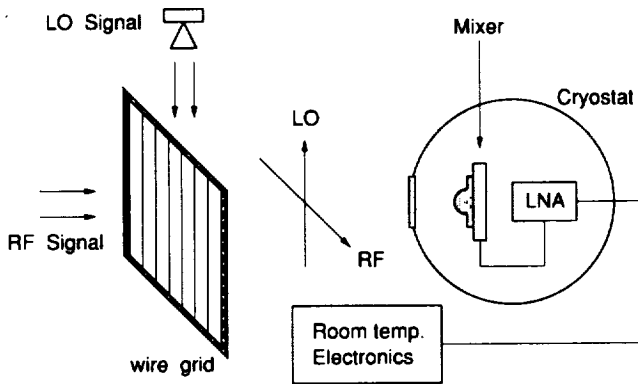
Fig. 5. Measurement setup for the balanced mixer. The LO frequency was 528 GHz and the cryostat temperature was 4.2 K.
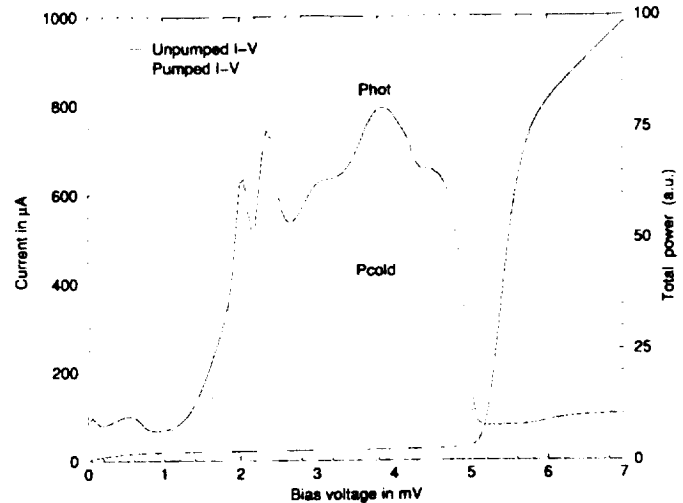
Fig. 6. Measured bias current and IF output power versus bias voltage at 4.2 K. The gap voltage is at 5.8 mV because two SIS junctions are connected in series. LO frequency for this measurement was 528 GHz and the measured DSB noise temperature was 105 K.

528 GHz, which means that the best noise temperature should be near this frequency.

IV. CONCLUSION

We have designed, fabricated and measured a quasi-optical balanced SIS mixer at 530 GHz using a cross-slot antenna. This is the first balanced mixer at this frequency range, and has excellent noise performance (105 K DSB). The RF optics and the IF circuits were not optimized, and we think that the performance could be improved further. Wider IF bandwidth is also possible through the use of a more sophisticated 180° hybrid design, perhaps integrated on-chip.

noise temperature of 5 K. The LNA output is sent to room temperature amplifiers and diode detectors which measure the total power in a 500-MHz IF bandwidth.

The noise temperature of the receiver was measured by the Y-factor method, using room temperature hot load and 80-K cold load. The cryostat temperature was 4.2 K for the measurements. The noise temperature reported here is referred to the input of the wire-grid; *no corrections have been made for the wire-grid or any other optical losses.* We adjusted the LO and the magnet current (which suppresses Josephson oscillations) to get a smooth IF output and then measured the noise temperature. Fig. 6 shows the pumped and unpumped I-V curves along with the IF outputs in a 500-MHz bandwidth at 528-GHz LO frequency when hot and cold loads are placed at the receiver input. At 528 GHz, the best noise temperature was measured to be 105 K. As mentioned earlier, for this device, the FTS measurement shows peak response at

REFERENCES

[1] S. A. Maas, *Microwave Mixers*, 2nd ed. Boston, MA: Artech House, 1993.

[2] A. R. Kerr and S.-K. Pan, "Design of planar image separating and balanced SIS mixers," *Proc. Seventh Int. Symp. Space Terahertz Technology*, Charlottesville, VA, Mar. 12–14, 1996, pp. 207–219.

[3] K. D. Stephan, N. Camilleri, and T. Itoh, "A quasioptical polarization-duplexed balanced mixer for millimeter wave applications," *IEEE/Trans. Microwave Theory*, vol. MTT-31, no. 2, pp. 164–170, Feb. 1983.

[4] C. E. Tong, and R. Blundell, "A self-diplexing quasioptical magic slot balanced mixer," *IEEE Trans. Microwave Theory Tech.*, vol. 42, pp. 383–388, Mar. 1994.

[5] G. Chattopadhyay and J. Zmuidzinas, "A dual-polarized slot antenna for millimeter waves," *IEEE Trans. Antennas Propagat.*, vol. 46, pp. 736–737, May 1998.

[6] G. Chattopadhyay, D. Miller, H. G. LeDuc, and J. Zmuidzinas, "A 550-GHz dual polarized quasioptical SIS mixer," in *Proc. Tenth Int. Symp. Space Terahertz Technology*, Charlottesville, VA, pp. 130–143, Mar. 16–18, 1999.

[7] M. Bin, "Low-noise THz niobium SIS mixers," Ph.D. dissertation, California Institute of Technology, Pasadena, Oct. 1996.

[8] J. R. Tucker and M. J. Feldman, "Quantum detection at millimeter wavelengths," *Rev. Mod. Phys.*, vol. 57, pp. 1055–1113, 1985.

[9] T. H. Büttgenbach, H. G. LeDuc, P. D. Maker, and T. G. Phillips, "A fixed tuned broadband matching structure for submillimeter SIS receivers," *IEEE Trans. Appl. Superconduct.*, vol. 2, pp. 165–175, 1992.

D   A Dual–Polarized Quasi-Optical SIS Mixer at 550 GHz

A Dual-Polarized Quasi-Optical SIS Mixer at 550 GHz

Goutam Chattopadhyay, *Member, IEEE*, David Miller, Henry G. LeDuc, and Jonas Zmuidzinas, *Member, IEEE*

Abstract—In this paper, we describe the design, fabrication, and the performance of a low-noise dual-polarized quasi-optical super-conductor–insulator–superconductor (SIS) mixer at 550 GHz. The mixer utilizes a novel cross-slot antenna on a hyperhemispherical substrate lens, two junction tuning circuits, niobium trilayer junctions, and an IF circuit containing a lumped element 180° hybrid. The antenna consists of an orthogonal pair of twin-slot antennas, and has four feed points, two for each polarization. Each feed point is coupled to a two-junction SIS mixer. The 180° IF hybrid is implemented using a lumped element/microstrip circuit located inside the mixer block. Fourier transform spectrometer measurements of the mixer frequency response show good agreement with computer simulations. The measured co-polarized and cross-polarized patterns for both polarizations also agree with the theoretical predictions. The noise performance of the dual-polarized mixer is excellent, giving uncorrected receiver noise temperature of better than 115 K (double sideband) at 528 GHz for both the polarizations.

Index Terms—Dual polarization, low noise, mixer, quasi-optical, superconductor–insulator–superconductor.

I. INTRODUCTION

DRAMATIC advances in millimeter- and submillimeter-wave receivers in recent years have resulted from the development of sensitive superconductor–insulator–superconductor (SIS) mixers, which now offer unsurpassed performance from 70 GHz to 1 THz. In principle, the sensitivity of SIS mixers is limited only by the zero-point quantum fluctuations of the electromagnetic field. In terms of the single-sideband (SSB) noise temperature, this limit is $h\nu/k_B \approx 0.05$ K/GHz. In practice, the SSB noise temperatures of the best SIS receivers now fall below 0.5 K/GHz over the 100–700-GHz band, dropping as low as 0.2 K/GHz in some cases.

For radio astronomy applications, one way to increase the sensitivity of SIS receivers further is to use a dual-polarized receiver. When both polarizations are received simultaneously, there is a $\sqrt{2}$ improvement in signal-to-noise *(S/N)* or a factor of two reduction in observing time. Dual-polarization operation can be achieved by using a wire-grid polarizer to split the telescope beam into two polarizations. The local oscillator (LO) can be injected using a beam splitter, either after the polarizer, in which case, two beam splitters are necessary, or before the polarizer, necessitating a single correctly oriented beam splitter. Either approach tends to lead to fairly complicated optical designs, especially for receivers with multiple bands or multiple spatial pixels. A much more elegant and compact solution is to directly construct a dual-polarization mixer. This is reasonably straightforward for quasi-optical designs since the receiving antenna is lithographically fabricated, and can be designed to receive both polarizations simultaneously. The slot-ring mixer is one such example where a single annular (circular or square-shaped) slot is used, which is fed at two points which are 90° apart, and which has been shown to provide good results at 94 GHz [1]. A slot-ring antenna could easily be adapted for use in an SIS mixer. One drawback for this antenna is that it has a broader radiation pattern (in angle) than the twin-slot antenna [2]. This is simply due to the fact that, at any given frequency, the transverse dimensions of a slot ring are smaller than those of a twin slot. This broader pattern of the slot ring will be somewhat more difficult to couple to, thus, the efficiency will be a bit lower than for a twin slot. However, we adapted the twin-slot antenna for dual polarization simply by crossing two sets of slots at 90°, as shown in Fig. 1. In this case, there are four feed points, as can be seen in the figure. The field distribution in the slots can be intuitively obtained from symmetry considerations. In particular, the field distributions in the vertical slots must be antisymmetric and, therefore, the voltage at the orthogonal ports (3, 4) must vanish. The characteristics of the cross-slot antenna have been calculated using the method of moments (MoM), and this design was found to have an excellent radiation pattern with fairly symmetric E- and H-plane beams, low impedance ($\approx 30\ \Omega$), wide bandwidth (the 1-dB impedance bandwidth for matching to a 30-Ω resistive load is about 40%), low cross polarization, and high coupling efficiency ($\approx 80\%$ for the co-polarized beam) [3].

II. MIXER DESIGN AND FABRICATION

To design an SIS mixer using the crossed-slot antenna, the easiest method would be to couple a separate tuned SIS circuit to each of the four antenna ports. One possible concern in this approach would be that the resonant frequencies of the four SIS circuits might not all be the same, which would lead to
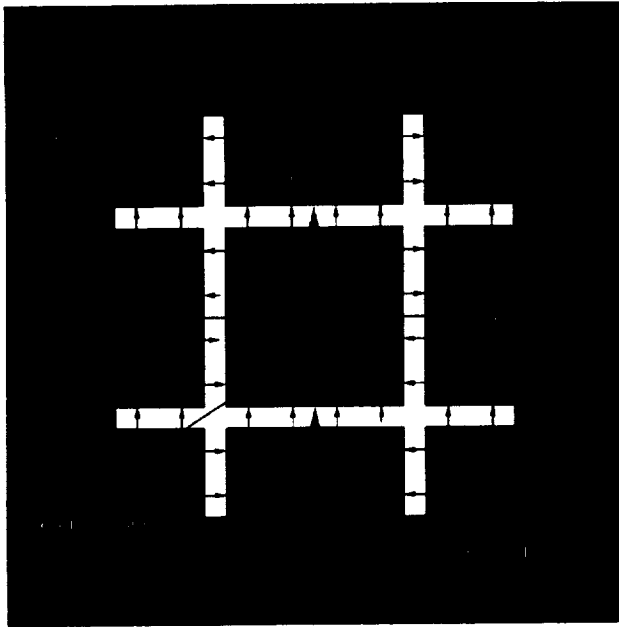
Fig. 1. Cross-slot antenna structure showing the field distribution in the slots when the two horizontal slots are excited symmetrically.
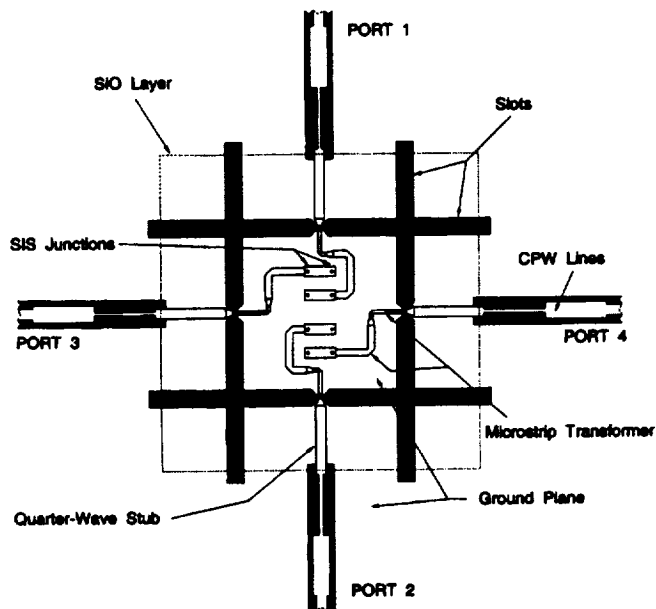

Fig. 2. Details of the mixer layout. CPW lines carry the IF output to the 180° hybrid. The junctions are placed as shown to allow suppression of the Josephson effect with a single magnet.

Fig. 3. Schematic showing how the two IF outputs for a given polarization are 180° out of phase. (a) Current flow for biasing the junctions in series. (b) Equivalent circuit.

Fig. 4. Simplified receiver layout. The elements within the Dewar are mounted on a 4.2-K cold plate.

degraded cross polarization and inferior performance overall. To minimize this effect, we decided to use tuning circuits in which the junction *separation* dictates the tuning inductance [4]. For two-junction tuning circuits, since both junctions are defined in the same lithography step, the tuning inductance is nearly immune to registration errors between layers. The four SIS circuits are combined into the two horizontal and vertical polarization outputs simply by biasing them in series from IF ports 1 to 2, and from ports 3 to 4. This also eliminates the necessity of attaching an electrical connection to the isolated ground plane at the center of the cross slot with the ground plane outside the slots. Fig. 2 shows the details of the mixer
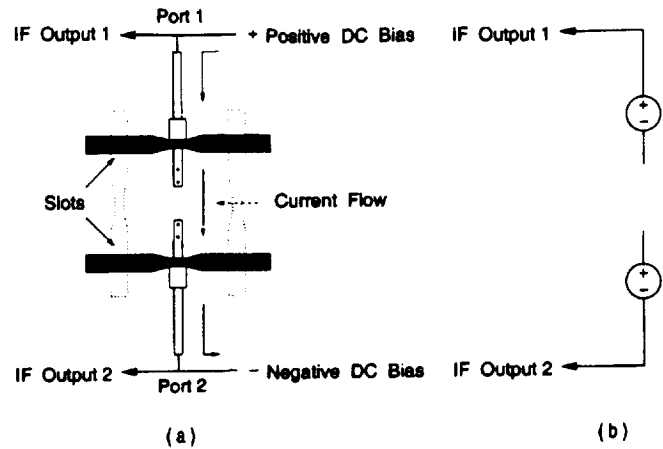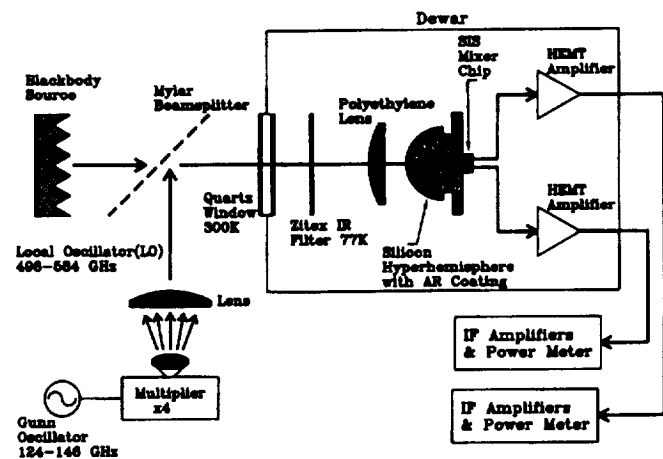
layout. The two-section microstrip transformer, shown in Fig. 2, allows a good impedance match between the antenna ($\approx 30\ \Omega$) and the tunnel junctions ($R_n/2 \approx 7\ \Omega$). The relatively low antenna impedance promotes good matching to even low resistance tunnel junctions. We used a simulation program, developed in house [5], to simulate and optimize the RF device performance.

We used the Jet Propulsion Laboratory's (JPL), Pasadena, CA, all optical-lithography junction fabrication process to fabricate junctions with three different junction areas: 1.44, 1.69, and 1.96 μm^2. Though the design was optimized for 1.69-μm^2 area junctions, we decided to fabricate three different junction area devices to allow for process variations. We used a three-mask-level Nb/Al–Oxide/Nb junction fabrication with a 2000-Å-thick niobium ground plane, 2500-Å-thick niobium wiring layer, and a single layer of 2000-Å-thick SiO, which is used as the dielectric for the superconducting microstrip line. The SIS mixer chip is placed on a hyperhemispherical silicon substrate lens. It can be seen from Fig. 2 that, for each polarization, there are two IF outputs and four SIS junctions, for a total of eight junctions on the chip. In principle, single-junction mixers could also be used, which would require only four junctions per chip.
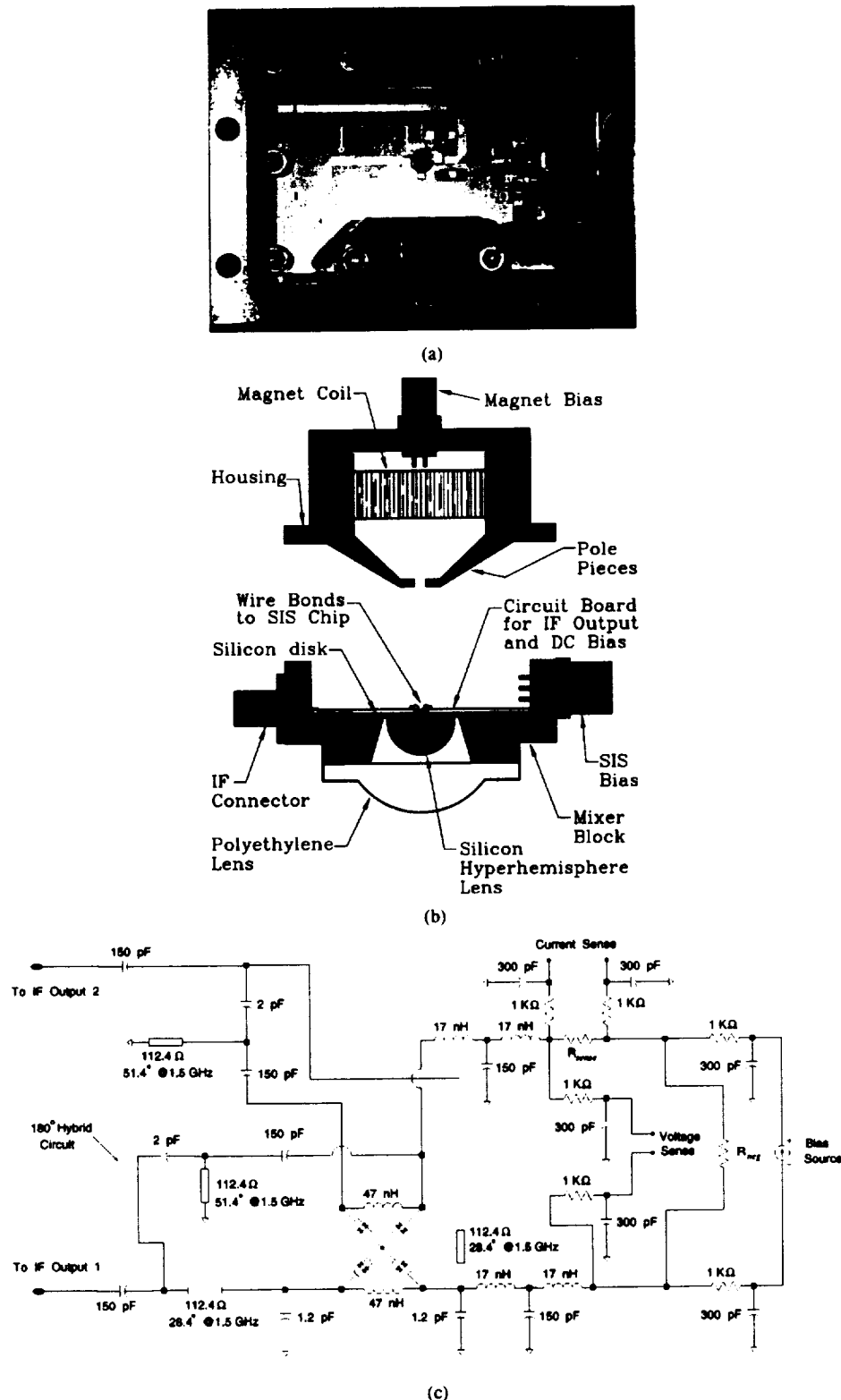
(a)

(b)

(c)

Fig. 5. Details of the mixer block and associated circuitry. (a) Block revealing the internal components. (b) Key to the hardware used within the block. (c) Details of biasing and IF circuits on the printed circuit board.

Due to the mixer structure and the series bias of the junction pairs, it turns out that the two IF outputs for a given polarization are 180° out of phase. This can be easily explained. For a given polarization [we choose the horizontal pair of slots, as shown in Fig. 3(a)], the LO and RF will have the same relative phase at either port (1 or 2), so we would expect the IF currents to be in

phase. However, due to the series biasing of the junctions, one junction pair is "forward" biased, while the other is "reverse" biased. As shown in the equivalent circuit in Fig. 3(b), the two IF outputs are 180° out of phase and, thus, a 180° hybrid is necessary to combine the two IF outputs for a given polarization. The hybrid circuit is designed using a first-order low-pass–high-pass
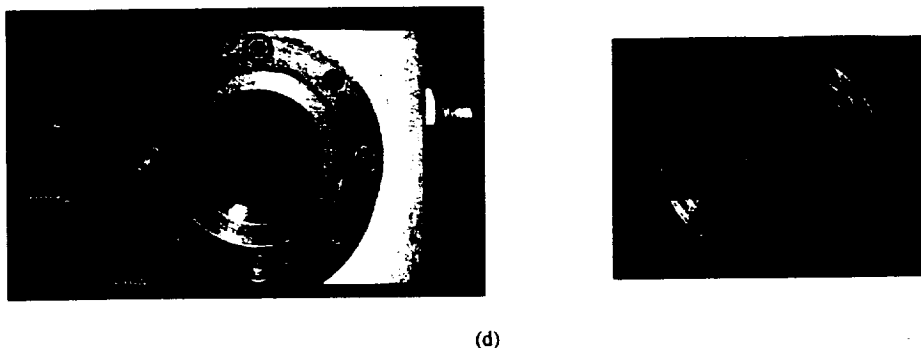
(d)

Fig. 5.   *(Continued.)* Details of the mixer block and associated circuitry. (d) Actual picture of an assembled block, with the polyethylene lens removed to show the AR coated silicon hyperhemisphere.

filter combination, whose 1-dB bandwidth at 1.5-GHz center frequency is more than 500 MHz. The hybrid is implemented using a combination lumped-element/microstrip circuit and is located inside the mixer block. The circuit was optimized using Hewlett-Packard's microwave design system (MDS) [6] to deliver maximum power to a 50-Ω load (the low-noise amplifier (LNA) input) from two 180° out-of-phase 30-Ω generators (the SIS IF outputs). The input reflection coefficient (S_{11}) of the lumped hybrid IF circuit was measured at cryogenic temperatures to evaluate its performance and to verify the design.

III. RECEIVER CONFIGURATION

A general view of the receiver configuration is shown in Fig. 4. The LO used is a tunable Gunn oscillator with a varactor multiplier [7], [8]. The RF and LO signals pass through a 10-μm-thick mylar beam splitter and the combined signals travel into the cryostat through a 3.8-mm-thick crystal quartz pressure window at room temperature, followed by a 0.1-mm-thick Zitex[1] IR filter at 77 K. Inside the cryostat, the well-collimated ($\approx F/17$) beam is matched to the broad beam pattern of the cross-slot antenna with a polyethylene lens and a silicon hyperhemispherical lens with antireflection (AR) coating of alumina-loaded epoxy[2] [9]. The quartz pressure window is AR coated with Teflon.

For the dual-polarization mixer, we used our existing single polarization mixer block, described in detail by Gaidis *et al.* [10], with some minor modifications, such as a second SMA connector to bring out two IF outputs for the two polarizations. Fig. 5 presents a detailed view of the mixer block and associated circuitry. Fig. 5(a) shows a disassembled block with the mixer chip at the center. Fig. 5(b) shows the hardware details for the mixer block and Fig. 5(c) shows the bias and IF circuitry. The back side of the SIS mixer chip is glued[3] to one side of a silicon support disk, and the silicon hyperhemisphere is glued to the opposite side of the disk. The SIS devices are fabricated on a 0.25-mm-thick 50-mm-diameter silicon wafer, which is then diced into 2.0 × 2.0 mm individual chips. The high resistivity (>1000 $\Omega \cdot$ cm) silicon support disk is 2.5 cm in diameter and 1.0-mm thick. The silicon hyperhemisphere is similar to the one described by Gaidis *et al.* [10].

[1]Zitex, Norton Company, Wane, NJ.

[2]Janos Technology Inc., Townshend, VT.

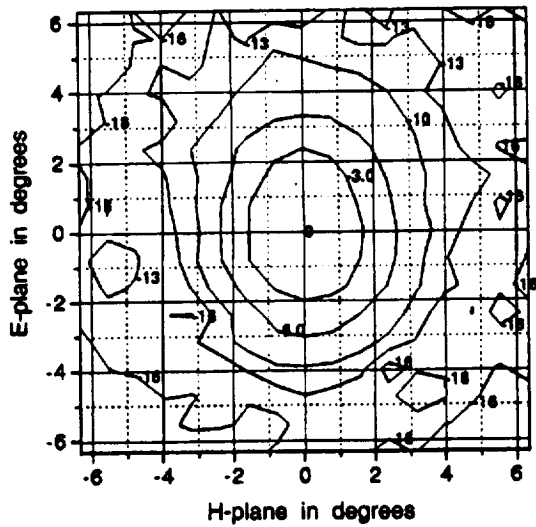[3]Litetak 3761 UV-curing adhesive, Loctite Corporation, Hartford, CT.

DC-bias supply and readout leads enter from the multipin connector on the right-hand sdie, and the mixer IF outputs, after being combined by the 180° hybrids, are carried on two different microstrip lines to SMA connectors on the left-hand side of the block. The schematic in Fig. 5(c) details the circuitry on the printed circuit board. The IF-blocking spiral inductors (17 nH) at liquid-helium temperature (4.2 K) add ≪1 Ω series resistance. The SIS mixer chip sits within a through hole at the center of the board, allowing straightforward wire bonding of the mixer chip to the biasing network and 180° hybrid circuits.

Fig. 5(d) shows the assembled mixer block, with the polyethylene lens removed to reveal the silicon hyperhemispherical lens. Semirigid coaxial cables connect the SMA IF output ports with HEMT LNAs. The measurements presented below were obtained using a 1.0–2.0-GHz LNA with measured noise temperatures of 5 K [11]. The LNA outputs are sent to room-temperature amplifiers and diode detectors, which measure the total power in a 500-MHz IF bandwidth.
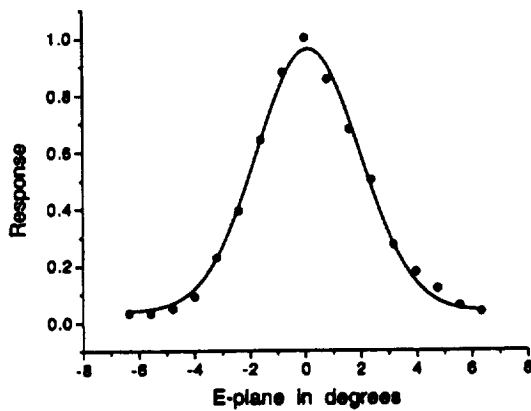
IV. MEASUREMENT AND RESULTS

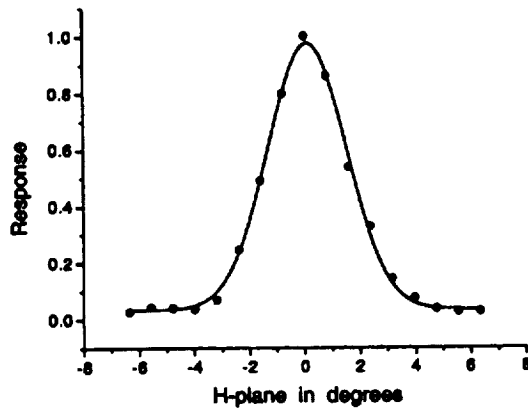### A. Antenna Beam-Pattern Measurements

The beam pattern of the dual-polarized antenna was measured with an antenna measurement system, which consists of an aperture-limited chopped hot–cold load on an x–z linear stage, stepper motors to drive the linear stage, a lock-in amplifier, and a data acquisition system [12]. The IF output of the mixer is detected, amplified, and fed to the lock-in amplifier. The hot–cold load linear stage was placed 24 cm away from the cryostat vacuum window for our beam pattern measurements. The hot–cold load aperture was set at 3.2 mm and the lock-in amplifier time constant was set at 3 s, giving signal to noise of about 18 dB for the measurement setup. The mixer was pumped with a 528-GHz LO source. The hot–cold RF signal and the LO were coupled to the junctions through a 10-μm-thick beam splitter. Fig. 6 shows the co-polarized beam pattern along with E- and H-plane cuts for the horizontal pair of slots. The E-plane beam is wider than the H-plane beam (as is expected) for both the polarizations. For the horizontal slots, the E- and H-plane full-width at half maximum (FWHM) was found to be 4.4° and 3.4°, respectively, giving E/H ratio of 1.3, which is higher than our theoretical prediction of 1.14. Similarly, for the vertical slots, the E- and H-plane FWHM was found to be 4.3° and 3.1°, respectively. The discrepancy between the measured

(a)

(b)

(c)

Fig. 6.   Antenna beam pattern for the horizontal pair of slots. (a) Contour plot. (b)–(c) E- and H-plane cuts for the beam. The LO frequency for the beam pattern measurement was set at 528 GHz.
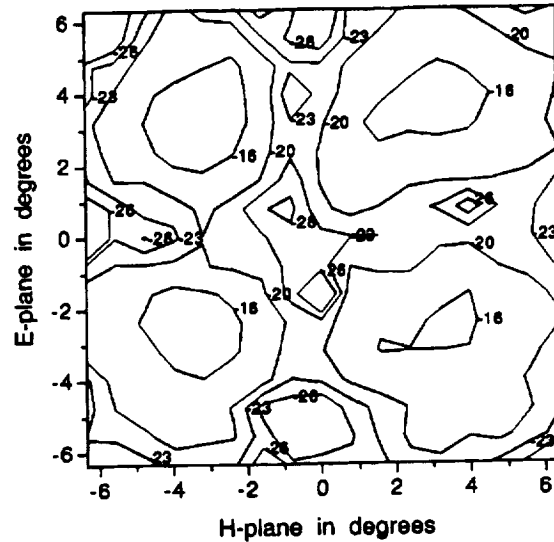

Fig. 7.   Cross-polarization beam pattern in decibels relative to peak co-polarized power. The LO frequency for the beam pattern measurement was set at 528 GHz.

distortion of the shape of the plastic lens at liquid-helium temperature (4.2 K). To verify that, we made measurements after rotating the plastic lens to different angles, but we did not notice any significant change in the beam pattern. We are currently developing better methods to align the chip with respect to the silicon lens.

For cross-polarization measurement, we used a wire-grid polarizer in front of the cryostat window. The hot–cold load aperture was set at 6.4 mm and the lock-in amplifier time constant was set at 10 s, which improved the S/N to about 28 dB. The cross-polarization beam pattern is shown in Fig. 7. One can see from the cross-polarization plot that the four lobes are not identical, and we suspect that this is due to the misalignment of the mixer chip. To verify this, we mounted another chip on the silicon hyperhemispherical lens, deliberately misaligning the chip with respect to the silicon lens. The resulting cross-polarization pattern indeed showed inferior cross-polarization performance, with the lower two sidelobes of Fig. 7 stretching more toward the bottom of the E-plane. That clearly demonstrated that the chip alignment plays a significant role in cross-polarization level of the beam. The integrated cross-polarization level was found to be around −15 dB (compared to the integrated co-polarized beam), which includes the effects of the wire-grid polarizer and beam splitter.

B. Fourier-Transform Spectroscopy

The receiver response as a function of frequency was measured with a Fourier-Transform spectroscopy (FTS) system built in-house using the mixer as a direct detector [13]. Fig. 8 shows the FTS response for two different polarizations of the receiver. The device we used for this measurement had 1.69-μm^2-area junctions and was optimized for 550-GHz frequency band. The FTS response agrees well with our simulation results, as can be seen from Fig. 8, given the nonidealities present in the measurement: strong water absorption lines at 557 and 752 GHz,

and calculated beamwidth ratio may be due to the misalignment of the mixer chip with respect to the silicon hyperhemispherical lens. It can be seen in Fig. 6(a) that the beam is stretched a bit toward the bottom end of the E-plane. This asymmetry is not expected theoretically and may be indicative of chip/lens misalignment. Initially, we thought that this could be the result of
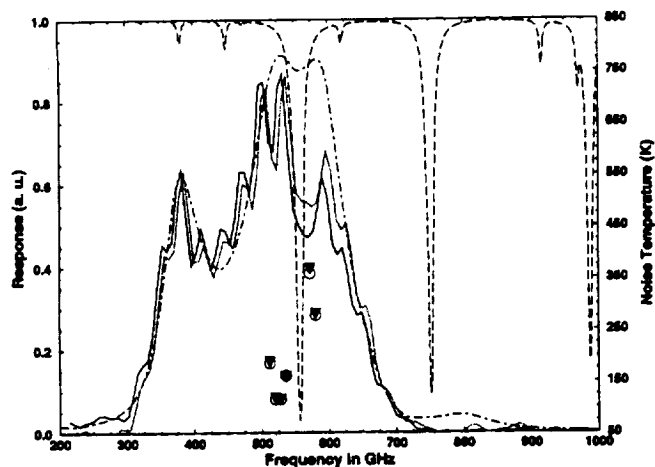
Fig. 8. FTS measured response along with the simulation results. The solid line is for the "horizontal" polarization and the dotted line is for the "vertical" polarization. The dotted–dashed line shows the simulated frequency response using nominal device parameters. The long dashed line shows the transmission of the FTS instrument. Also shown are the mixer noise temperatures as a function of frequency, the circles are for the "horizontal" polarization, and the triangles are for the "vertical" polarization.
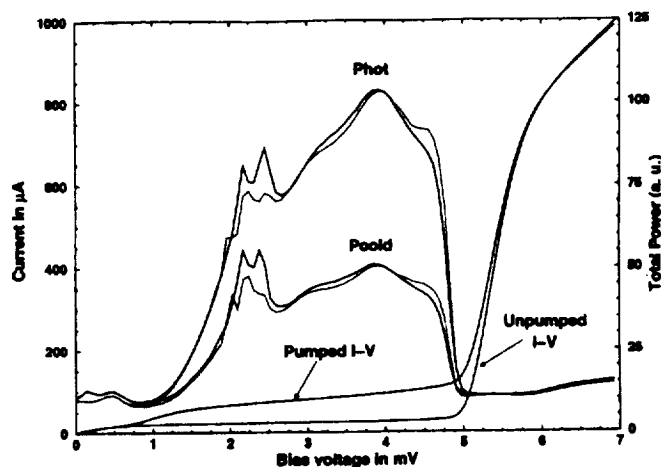

Fig. 9. Current and IF output power versus bias voltage at 4.2 K when we measured both the polarizations simultaneously. The solid lines are for the "horizontal" polarization and the dotted lines are for the "vertical" polarization. The LO frequency for both polarization was 528 GHz and the measured DSB receiver noise temperatures were 115 K. The LO pumped and unpumped *I–V* curves actually plotted for both polarizations, but are indistinguishable on this scale.

and Fabry–Perot resonances from the IR filter spaced approximately 50 GHz apart. The FTS response is very similar for both the polarizations, and the peak response was found at 528 GHz, which means that the best noise temperature for these devices would be around this frequency.

C. Heterodyne Measurements

We measured the noise temperature of the receiver, with both the polarizations simultaneously active, using the Y-factor method. The cryostat temperature was 4.2 K for all the measurements. The noise temperatures reported here are referred to the input of the beam splitter; *no corrections have been made for beam splitter or any other optical losses.* We mounted the device at 45° angle with respect to the horizontal microstrip line shown in Fig. 5(a). The junctions were biased, as shown in Fig. 5(c), where the IF outputs of the two different polarizations are isolated from each other by two 47-nH spiral inductors. A single LO source pumped the junctions for both the polarizations simultaneously. It was very important to check that we indeed were observing dual-polarization operation, and we confirmed that experimentally. We placed a wire-grid polarizer in between the beam-splitter input and a cold load (80 K). As we rotated the grid about the optical axis, the two IF outputs were observed to increase or decrease independently, depending on whether the corresponding mixer could *see* the cold load behind the wire gird. This clearly demonstrated that the mixer was operating in dual-polarization mode.

We adjusted the LO and magnet current to get a smooth IF output for both the polarizations and then measured the noise temperature. Fig. 9 shows the pumped and the unpumped *I–V* curves along with the IF outputs in a 500-MHz bandwidth at 528-GHz LO frequency when hot and cold loads (absorber at room temperature and 80 K, respectively) are placed at the receiver input. The pumped *I–V* curves clearly show the photon step around $V \approx 1.4$ mV, as expected from a 528-GHz LO

source ($h\nu/e \approx 2.2$ mV). Since the junctions are in series, the gap voltage is at 5.8 mV and the photon step will appear at 5.8 mV $- 2 \times 2.2$ mV $= 1.4$ mV. We measured nearly identical double-sideband (DSB) noise temperature of 115 K for both the polarizations at 528 GHz. The mixer noise temperature as a function of frequency was found to be very similar for both the polarizations and is shown in Fig. 8.

V. CONCLUSION

We have designed, fabricated, and measured a dual-polarized quasi-optical SIS receiver at 550 GHz using a cross-slot antenna structure on an antireflection coated hyperhemispherical silicon lens, which gives excellent noise temperature performance (115-K DSB) for both of the polarizations. The measured antenna radiation patterns agree reasonably well with theoretical predictions. We have shown that this receiver has almost identical performance for both the polarizations and could be very effectively used for submillimeter radio astronomy observations. Wider IF bandwidths are possible through the use of a more sophisticated 180° hybrid design, perhaps integrated on-chip. It is also possible to use this device as a balanced mixer [14].

REFERENCES

[1] S. Raman and G. M. Rebeiz, "Single- and dual-polarized millimeter-wave slot-ring antennas," *IEEE Trans. Antennas Propagat.*, vol. 44, pp. 1438–1444, Nov. 1996.

[2] J. Zmuidzinas and H. G. LeDuc, "Quasi-optical slot antenna SIS mixers," *IEEE Trans. Microwave Theory Tech.*, vol. 40, pp. 1797–1804, Sept. 1992.
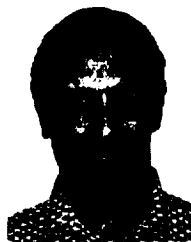
[3] G. Chattopadhyay and J. Zmuidzinas, "A dual-polarized slot antenna for millimeter waves," *IEEE Trans. Antennas Propagat.*, vol. 46, pp. 736–737, May 1998.

[4] J. Zmuidzinas, H. G. LeDuc, J. A. Stern, and S. R. Cypher, "Two-junction tuning circuits for submillimeter SIS mixers," *IEEE Trans. Microwave Theory Tech.*, vol. 42, pp. 698–706, Apr. 1994.

[5] M. Bin, "Low-noise THz niobium SIS mixers," Ph.D. dissertation, Dept. Phys., California Inst. Technol., Pasadena, CA, Oct. 1996.

[6] "*Microwave Design Systems (MDS), Version mds.07.10*," Test and Measurement Organization, Hewlett-Packard Company, Palo Alto, CA.

[7] J. E. Carlstrom, R. L. Plembeck, and D. D. Thornton, "A continuously tunable 65–115 GHz Gunn oscillator," *IEEE Trans. Microwave Theory Tech.*, vol. MTT-33, pp. 610–619, July 1985.

[8] N. R. Erickson, "High efficiency submillimeter frequency multipliers," in *IEEE MTT-S Int. Microwave Symp. Dig.*, Dallas, TX, May 1990, pp. 1301–1304.

[9] J. Zmuidzinas, N. G. Ugras, D. Miller, M. C. Gaidis, H. G. LeDuc, and J. A. Stern, "Low-noise slot antenna SIS mixers," *IEEE Trans. Appl. Superconduct.*, vol. 5, pp. 3053–3056, June 1995.

[10] M. C. Gaidis, H. G. LeDuc, M. Bin, D. Miller, J. A. Stern, and J. Zmuidzinas, "Characterization of low-noise quasi-optical SIS mixers for the submillimeter band," *IEEE Trans. Microwave Theory Tech.*, vol. 44, pp. 1130–1139, July 1996.

[11] J. W. Kooi, private communication, Sept. 1998.

[12] D. A. Miller, "Comparison between theory and measurement of beam patterns for double-slot quasi-optical SIS mixers," M.S.E.E. thesis, Dept. Elect. Eng., California State Polytech. Univ., Pomona, CA, 1998.

[13] Q. Hu, C. A. Mears, P. L. Richards, and F. L. Lloyd, "Measurement of integrated tuning elements for SIS mixers," *Int. J. Infrared. Millim. Waves*, vol. 9, pp. 303–320, 1988.

[14] G. Chattopadhyay, F. Rice, D. Miller, H. G. LeDuc, and J. Zmuidzinas, "A 530-GHz balanced mixer," *IEEE Microwave Guided Wave Lett.*, vol. 9, pp. 467–469, Nov. 1999.

David Miller was born in Portsmith, VA, on May 1, 1959. He received the B.S. degree in electrical engineering and the M.S.E.E. degree from the California State Polytechnic University, Pomona, in 1990 and 1998, respectively.

He is currently an Associate Engineer in the Submillimeter Group, California Institute of Technology, Pasadena. His primary responsibilities have involved the development of quasi-optical SIS receivers for submillimeter astronomy from the Kuiper Airborne Observatory and Caltech Submillimeter Observatory. His research interests include characterization and measurements of antenna patterns and their associated optics. He is currently involved in wide-band IF receiver development for extra-galactic astronomy.

Henry G. LeDuc was born in Butte, MT, on March 8, 1955. He received the B.S. degree in physics from Montana State University, Bozeman, in 1977, and the Ph.D. in physics from the University of California at Davis, in 1983. His thesis work involved far-infrared spectroscopy of solid-state ionic conductors.

He is currently a Group Leader at the Jet Propulsion Laboratory, California Institute of Technology, Pasadena, where his group develops SIS tunnel junctions for heterodyne receivers.

Goutam Chattopadhyay (S'93–M'99) received the B.E. degree in electronics and telecommunication engineering from the Bengal Engineering College, Calcutta University, Calcutta, India, in 1987, the M.S. degree in electrical engineering from the University of Virginia, Charlottesville, in 1994, and the Ph.D. degree in electrical engineering from the California Institute of Technology, Pasadena, in 1999.

From November 1987 to December 1992, he was a Design Engineer at the Tata Institute of Fundamental Research (TIFR), Pune, India, where he designed local-oscillator systems for the Giant Meterwave Radio Telescope (GMRT) Project. In January 1993, he joined the Electrical Engineering Department, University of Virginia. In September 1994, he joined the California Institute of Technology, where he is currently with the George Downs Laboratory of Physics. His research interests include microwave and millimeter-wave receivers, antennas, SIS mixer technology, and frequency multipliers.

Dr. Chattopadhyay is a member of Eta Kappa Nu. He received the 1987 Best Undergraduate Student Gold Medal presented by Calcutta University, the 1992 Jawaharlal Nehru Fellowship Award presented by the Government of India, and the 1997 IEEE MTT-S Graduate Fellowship Award.

Jonas Zmuidzinas (M'91) was born in Duarte, CA, on September 8, 1960. He received the B.S. degree in physics from the California Institute of Technology, Pasadena, in 1981, and the Ph.D. degree in physics from the University of California at Berkeley, in 1987. His doctoral dissertation described the development of a laser heterodyne receiver for airborne astronomy in the far-infrared field (800–2000 GHz).

From 1988 to 1989, he was a Post-Doctoral Fellow at the University of Illinois at Urbana-Champaign, where he was involved with the design and fabrication of SIS mixers. He is currently a Professor of physics at the California Institute of Technology. His research interests are in the areas of high-frequency superconducting devices and their application to submillimeter astronomy.